國立臺灣大學醫學院暨工學院醫學工程學研究所

碩士論文

Graduate Institute of Biomedical Engineering

College of Medicine and College of Engineering

National Taiwan University

Master Thesis

探討交感神經提供易活化毛囊幹細胞的環境

Sympathetic nerve provides a permissive niche for hair follicle stem cell activation

黃海恩

Hai-En Huang

指導教授：林頌然 博士

Advisors: Sung-Jan Lin, M.D., Ph.D.

中華民國106年 7月

July, 2017

doi:10.6342/NTU201701146

口試委員會審定書

國立台灣大學碩士班學位論文

口試委員審定書

探討交感神經提供易活化毛囊幹細胞的環境

Sympathetic nerve provides a permissive niche for hair follicle stem cell activation

本論文係黃海恩君（r04548065）在國立台灣大學醫學工程研究所完成之碩士學位論文，於民國106年07月04日承下列考試委員審查通過及口試及格，特此證明

口試委員：林頌然（簽名）

（指導教授）

謝松蒼

陳志強

所長：黃義侑（簽名）

中文摘要

交感神經突觸會生長進入皮膚並與毛囊和一旁的豎毛肌纏繞形成最簡單的豎毛單元。透過分泌正腎上腺素，交感神經得以促使毛髮站立來增大動物的體型並且調控溫度。在毛髮生長週期中，交感神經的纖維會表現出消長的現象，在進入生長期前期時增加，當進行到中期到後期這段時間開始減少。而在角質細胞中，正腎上腺素會有抑制細胞分裂並刺激細胞分化的作用。在人體身上使用乙型 2 型腎上腺素受體抑制劑發現有掉髮的現象，由此暗示交感神經擁有可以影毛髮生理恆定的能力。

在我們的研究中發現，交感神經跟毛囊突隆區有距離相當近的交集。交感神經纖維在生長期前期均勻地在整片背皮中分佈，並且有其密度有上升的現象。而在使用六羥多巴胺除掉交感神經後，毛囊從休止期進入生長期、和生長期前期進入生長期後期的過程會被阻斷，但是如已經進入生長期後期則沒有影響。使用乙型腎上腺素受體促進劑（異丙腎上腺素）可以刺激毛髮提前進入生長期。從我們的結果得知交感神經在自然進入生長期的生長期前期中扮演重要角色。我們更進一步分離出毛囊幹細胞來探討交感神經移除與不移除對於基因表現的變化。其中 Wnt 信號並不會受到交感神經得去除的影響。然而，Gli1 和 Gli2 的信號在交感神經去除後很顯著的表現有下降的情況，這很可能是交感神經可以透過刺激生成 hedgehog 信號來活化毛囊幹細胞。但在知道交感神經並不會分泌 Shh 訊號的情況下，我們認為交感神經可能透過其他方式來調控 hedgehog 在毛囊的表現。

關鍵字：交感神經、毛囊生長週期、異丙腎上腺素、乙型腎上腺素受體、環孢素

doi:10.6342/NTU201701146

Abstract

The sympathetic nerve innervates in the skin and associates with hair follicles and arrector pili muscles to assemble the piloerection units. Through secretion norepinephrine, the sympathetic nerves system can trigger piloerection to expand body size and mediate body temperature. During hair cycle, the sympathetic nerve fibers oscillate with hair cycle phase which increases at the early anagen but decreases at the mid-anagen to the regression stage in the hair follicles. Treatment with norepinephrine can inhibit keratinocyte proliferation and trigger cell differentiation. The administration of adrenoceptor antagonist propranolol will lead to hair loss in the human which imply the sympathetic nerves may involve in hair follicle homeostasis regulation.

In our study, we identify that the sympathetic nerve closely associates with bulge region of the hair follicle. The neuron fibers density increases and homogeneously distributes in the interfollicular regions of the back skin at the early anagen phase. The 6-hydroxydopamine induced sympathectomy block telogen-to-anagen transition, early anagen I-to-anagen III transition, but not full anagen progression. Beta-adrenoceptor agonist, isoproterenol, can induce an early hair cycle progression. In our result, the sympathetic nerve is important in the early spontaneous hair cycle entry. We further isolate the hair follicle stem/progenitor cells (HFSC) and identify the gene expression profile in sympathectomy and non-sympathectomy skin. The Wnts expression is not affected after sympathectomy. However, the gli1, gli2 significantly decrease in hair follicle stem cells after sympathectomy which indicates that sympathetic nerves can activate HFSC through activating hedgehog signaling. Furthermore, no study showed SN can secrete Shh. Therefore, we conclude that sympathetic nerves can mediate hair cycle through the alternative pathway by mediating the hedgehog pathway.

Key words: sympathetic nerve, hair cycle, beta-adrenoceptor, isoproterenol, cyclosporine

doi:10.6342/NTU201701146

Index

doi:10.6342/NTU201701146

doi:10.6342/NTU201701146

doi:10.6342/NTU201701146

Tables of figures

doi:10.6342/NTU201701146

doi:10.6342/NTU201701146

TABLE OF TABLES

doi:10.6342/NTU201701146

Chapter 1 Introduction

1.1 Introduction of skin

Skin is the biggest organ in human body. It performs several important functions: protection from pathogen, sensation, thermoregulation, evaporation, storage lipid and water, and water resistance. The structure of skin can be divided into epidermis, dermis, and hypodermis. (Figure 1.1).

Epidermis is located at the top position of the skin and shows a laminated structure. It includes, beginning with the innermost layer, stratum basale, stratum spinosum, stratum granulosum, stratum lucidum, and stratum corneum (1). Stratum basale is the site where keratinocytes proliferate, then moves upward. Melanocytes also reside in stratum basale. Keratinocytes form desmosomes to anchor with each other in stratum spinosum (1). Some nerve endings penetrate into this layer (1). Keratinocytes lose their nuclei and organelles and secrete lamellar body, contains lipid and protein, into extracellular space to render the water-proof property in stratum granulosum. Stratum corneum, composed of tightly packed dead cells, acts as the first line of the innate immune defense and prevents water loss from the body. Though keratinocytes are the most abundant cells in the epidermis, Merkel cells, and Langerhans cells are also present (1).

Dermis lies beneath the epidermis and structurally can be divided into two regions: papillary region and reticular region. Papillary and reticular regions are defined by two tissue composition, which are loose and dense connective tissue respectively. Dermis harbors blood vessels, mechanoreceptors, thermoreceptors, and lymphatic vessels. It

doi:10.6342/NTU201701146

also contains many important accessory organs: arrector pili muscle, hair follicles, eccrine glands, apocrine glands, and sebaceous glands (2, 3).

The hypodermis is also known as subcutaneous tissue. It is constituted by adipocytes, macrophages, and fibroblasts. With the resident of adipocytes, skin acquires the ability to be an insulator to keep the body warm.

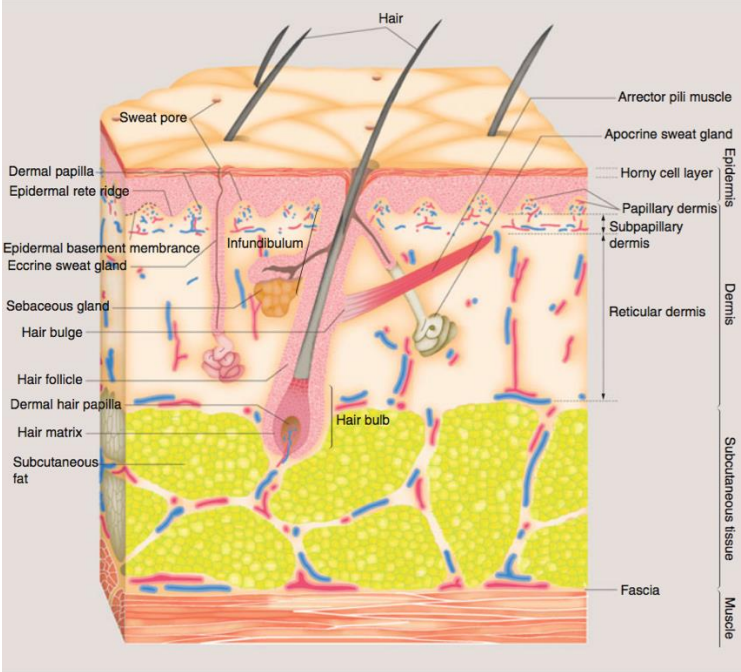

Figure 1.1 Skin structure (2)

1.2 Introduction of hair follicles

The hair follicle is the smallest organ in the skin. It is derived from the epidermis. In the embryo of the mouse, clubs of undifferentiated epidermis cells proliferate, migrate downward and wrap the mesenchymal cells to form hair follicles. Several stem cells reside in the hair follicle rendering the ability of cyclic regeneration. Hence, the structure of hair follicles changes through the different stages of the hair cycle (3-6).

doi:10.6342/NTU201701146

1.2.1 Hair follicle structure

From a sagittal view, a hair follicle, in anagen, can basically be divided into four parts. Starting from distal, it is infundibulum, isthmus, supra-bulbar region, and bulb. The infundibulum is the region where keratinocytes won't proliferate. The end of infundibulum is where sebaceous gland duct inserts into the hair follicle. Below the infundibulum, the isthmus is joined. Epithelial stem cells reside in the lower isthmus, also called bulge. Arrector pili muscle is inserted into this region as well. The supra-bulbar region connects the bulb and isthmus. Anagen bulb is highly proliferative due to the resident of activated keratinocytes where is named matrix. From an axial view, the structure of the hair follicles is constructed with several concentric circles. The part in the middle is the hair shaft (HS), the part grows out of the body. Then, it is followed by, from innermost to the outermost, inner root sheath (IRS), outer root sheath(ORS) (7), and the connective tissue sheath (CTS) (Figure1.2).

1.2.2 Hair cycle (stem cell behavior)

Hair follicle contains two main cell population where is highly proliferative. One locates at the mid of the follicle, around the bulge region. A group of cells locates beneath the sebaceous gland and close to the arrector pili muscle attached site. They are called the hair follicle stem cells (HFSCs) (8). HFSCs has been overserved in involving in hair follicle elongation in the hair growth. Its duplicated cells migrate down to the upper bulb and proliferate to form the ORS (8, 9).

The other group of the proliferative cells has been observed beneath the bulge region of the hair follicle. It contacts with the hair bulge on the one side and the DP on the other(8, 10). This population was named germ cells. When the hair cycle begins, these

doi:10.6342/NTU201701146

cells will be activated by the DP with FGF, Wnt signalings (10). Then it activate the HFSCs to proliferate (8).

In catagen phase, the structure of bulb shrink since the cells in the bulb begin apoptosis. With the massive apoptosis in the hair follicles, a dystrophy structure of hair follicles can be observed. In the end of catagen, the original hair follicle retracts and form the bulge region (11). In telogen phase, no supra-bulbar and bulb region can be observed, the hair follicle stem cells keep in quiescence stage in bulge region of hair follicle. A small club of keratinocytes attached to the bugle region, called hair germ (HG). Furthermore, a tiny ball like composition of differentiated fibroblast cells under HG is called dermal papilla (DP), responsible for hair growth induction (4-6).

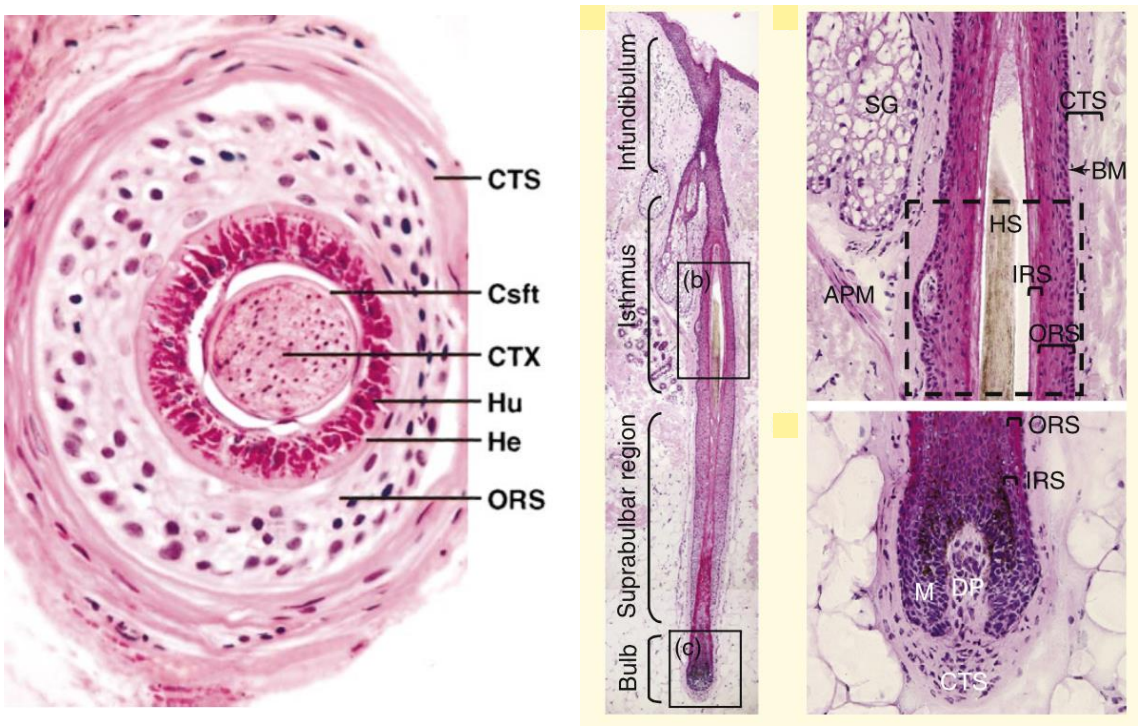

Figure 1.2 Structure of hair follicle (5)

doi:10.6342/NTU201701146

The hair cycle can be divided into three distinct phases: the elongation phase, anagen, the regression phase, catagen, and the rest phase, telogen (Figure1.3). Anagen can be subdivided into 6 stages, anagen I to VI. At anagen I, the stem cells in HG start proliferating and expand the size of the HG (12-14). At the anagen II, the enlarged part of HG engulfs the DP which forms the bulb. In this stage, the epithelial cells re-organize and differentiate in the contact with DP (15). Epithelial stem cells in HG are turning to matrix cells and rapidly proliferating to form the IRS and HS in anagen III. The stem cells in the bulge, then, migrate and proliferate downward to form the ORS giving the hair follicles to elongate (9, 16, 17). The hair follicles and hair rapidly extend at anagen III to VI. When the HS penetrates out of the skin, the stage is defined as anagen VI (5, 18, 19).

At the end of the anagen, the proliferation of matrix is arrested and the transition of elongation to regression(catagen) takes place. Due to the massive apoptosis, the size of bulb presumably shrinks and ORS begins to actively degenerate in the results of retracting DP upwards to the bottom of the bulge. In the research, TUNEL is the prime indicator for anagen-catagen transition and catagen progression. It can be subdivided into eight stages in the catagen depending on the number of TUNEL expression cells in the bulb (5, 19).

At the rest phase(telogen), some ORS cells survive from the aggressive apoptosis event in the regression stage resemble the new bulge and HG. The old HS forms a club hair who is anchored in an inner quiescence bulge cell layer expressing Keratin 6 (5, 19, 20).

doi:10.6342/NTU201701146

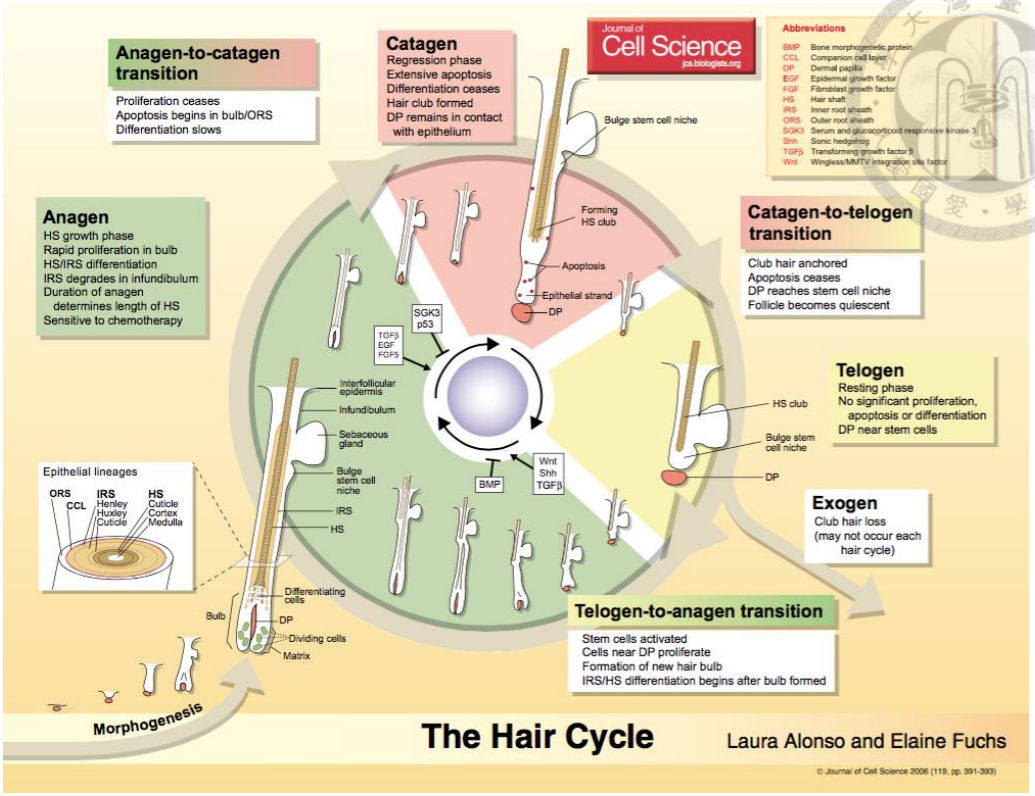

Figure 1.3 Hair cycle (20)

doi:10.6342/NTU201701146

Hair growth is a cyclic event. In C57BL/6, or called B6, mice, it has been unveiled that hair growth simultaneous occurs in the different individuals in the first two cycles. After birth, the first anagen takes place at 4-week-old. The hair cycle proceeds for two weeks and follows with the catagen phase for another one week. The hair follicles rest in telogen phase and will initiate next anagen after 5 weeks (Figure 1.4). Intriguingly, the hair cycle schedule might be variant from the different environmental conditions, such as humidity, light exposure time, temperature, breeding condition etc (19).

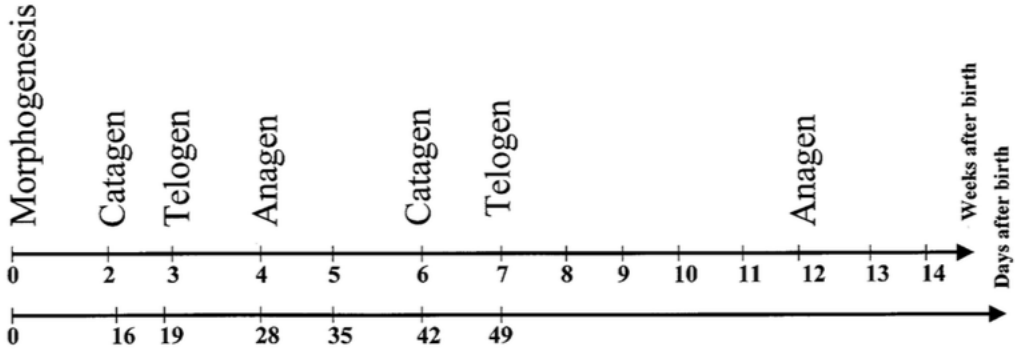

Figure 1.4 Timescale of hair cycle in C57BL/6 mice ***(19)***

The hair has two different growth pattern: synchronized hair growth and the hair wave (21, 22). In the young mice, their first 2 hair cycle is almost synchronized in the same time that can be observed from the skin. However, after the 2nd postnatal hair cycle, the hair growth pattern goes in a wave-like procession. The hair growth starts on the anterior venter, and it proceeds to the posterior, then the hair growth from the venter to the dorsum until the hair wave coalesce, finally, the hair wave propagates from posterior to anterior on the dorsum (22).

doi:10.6342/NTU201701146

1.2.3 Modulation of hair follicle stem cells by the micro- and macro-environment

In previous studies, several signaling pathways, including BMP, Wnt, FGF-18, TGF-ß, govern and regulate the stem cells responsible for the hair cycle (23-29). The studies have shown the high expression of BMP-6 and FGF-18 in Keratin 6+ inner bulge layers restricts the hair follicles in the resting stage (9). When entry the late telogen, DP secreted FGF-7, FGF-10, TGF-ß2, and noggin to trigger hair germ cells activation (12). After the activating Wnt signal overcomes the suppressing BMP signal, the hair follicles enter anagen. All the mentioned signals interact within the hair follicle is regarded as the microenvironment regulation. Nevertheless, in recent studies, it has been discovered that signals from the outside of hair follicle, the macro-environment can regulate the hair growth. There are a few macro-environment sources are being discussed: adipocytes, immune cells, hormone, circadian, nerve system, aging, etc (6). Further studies are investigating how these sources influence the stem cells activity within follicles (6).

Adipocytes

The adipocyte progenitor cells and mature adipocyte compose the subcutaneous layer of the skin, and the adipocyte populations change following the hair cycle (30). Actually, the subcutaneous adipocytes not only function in thermo-regulation, and protection from the collision, but also secrete BMP2 or PDGFa to influence the hair growth. The mature adipocytes were discovered to express the BMP-2 which keep the niche in quiescence (24). The latest study points out the adipocyte precursor cells(APCs) is required to promote the hair growth. The PDGF secreted from the APCs induces anagen entry (7).

doi:10.6342/NTU201701146

Neurons (sensory and SN)

Both sensory and sympathetic nerve (SN) innervates at hair follicle (31). Sensory nerve endings wrap around constructing a crown-like structure above the bulge area where express Gli1 (32). The expression of Hh signaling from sensory nerve ending contributes to hair regeneration (33-35). Sympathetic nerve climbs along the arrector pili muscle whose one end anchors at the bulge. Although the role of sympathetic nerves in regulating hair regeneration is still unknown, patients taking the propranolol (beta-receptor antagonist) could develop alopecia, it implied that the sympathetic nerves are also involved in hair cycle regulation (36). In the animal experiments, the skin hair displayed a slower growth rate after surgical nerve truncation in the dog (37) and chemical sympathectomy in mice (38, 39). Alternatively, chemical sympathectomy accelerates the hair growth in another study (40). Hence, the role of SN on the hair regeneration in the niche still need to be elucidated.

Immune system

Immune cells may be involved in the hair regeneration was indicated in the recent studies (41-43). The number of macrophages dramatically decrease in late telogen to early anagen transition. In this transition pahse, the vast amounts of Wnt factors (Wnt 7b, Wnt10a) are released from apoptic macrophage to trigger the canonical Wnt/ ß -catenin pathway and activate hair follicle stem cells to promote anagen entry (41).

The regulatory T (Treg) cells has been unveiled that it is involved in few tissues activities, including lung, fat and skin (44-46). Treg dominantly localize around the HFSCs. It has been investigated to be associated with the depilation-induced hair growth. With the depletion of the Treg in the skin, the hair won't grow after the depilation procedure. Treg was believed to mediate the hair growth through the

doi:10.6342/NTU201701146

secretion of the Jagged 1 since the exogenous Jagged 1 can retrieve the hair growth after the Treg depletion in the skin (42).

1.3 Hair cycle induction

Except for the time or seasonal control of hair cycle, the other way to induce the hair growth includes the chemical and physical methods.

1.3.1 Plucking

Evidence showed that new hair and vibrissae emerge after plucking (47, 48). Plucking also shows the superiority to shaving and clipping on hair growth induction (49). To understand the effect of the plucking on the hair cycle induction. Female C57BL/6 mice were used as the standard model. The time-scale of induced hair cycle and change of the pigmentation has been created (19). It suggests the skin turns gray from pink on day five after depilation and the induced hair follicles reach full anagen (anagen VI) on day 12 after plucking. Catagen occurs on day 17 after depilation when the gray color of the skin can be observed. The cycle returns to telogen on day 21 after depilation (19).

The effect of the plucking on the hair growth induction was hypothesized to be related to the Keratin 6+ inner layer of bulge who secrete vast quantities of BMP suppression signals (9). The end of the club hair anchors in this population. With the club hair removed, the inner cell layer is devastated leading to the dramatic plunge of BMP signals. The level of activating Wnt signal suddenly surpasses the BMP suppression threshold. Hair follicles proceed to the precocious telogen phase (9, 24).

doi:10.6342/NTU201701146

Plucking has later been used to study the inhibition signaling in the regulation of the hair cycle entry and became the model in the control of the onset of the hair growth (24).

1.3.2 Cyclosporin A (CsA)

Cyclosporin A(CsA), an immunosuppressant drug, has recently been appreciated as a modulatory agent in hair growth induction and hair regression suppression. Few studies have demonstrated that either intraperitoneal or topical administration of CsA can stimulate the hair growth in C57BL/6 mice and nude mice (50, 51). CsA was also discovered to promote the mouse vibrissae follicles to grow in organ culture (52). On the other side, CsA is also an agent in blocking the chemotherapy-induced catagen and dexamethasone-induced catagen (53, 54). However, topical application of CsA exhibits limited hair growth in the human alopecia. The difference was suggested to be related to the synapse associate protein 102 (SAP102) which isn't expressed in human skin but is induced to express in the ORS region of mouse anagen hair (55). Subsequent studies focus on the possible mechanisms of CsA on both promoting hair growth and inhibiting catagen development. It has been investigated that CsA increase the mRNA expression of vascular endothelial growth factor (VEGF), hepatocyte growth factor (HGF), and nerve growth factor (NGF) in the vibrissae follicles (52). CsA was found to be the inhibitor of calcineurin. Inhibition of calcineurin lowers the differentiation markers level in mouse hair keratinocytes due to the inhibition of nuclear factor of activates T cells (NFAT) nuclear translocation. Subsequently, the anti-apoptotic factors Bcl-2 increases which prevent the follicle cells from massively apoptosis and growth factors IL-1 upregulates to promote the hair elongation in both nude and C57BL/6 mice (50, 56). Last but not least, CsA suppresses the apoptosis event by operating the caspase-

doi:10.6342/NTU201701146

dependent and AIF-dependent pathways. CsA was discovered to prevent cytochrome c release from the mitochondria under mitochondrial membrane permeability regulation and, therefore, block the caspase-dependent pathway. On the other side, CsA antagonizes to cyclophilin A (CypA), which cleave the nuclear DNA into small pieces after interacting with flavoprotein, apoptosis-inducing factor (AIF) (57-62).

With the property that the CsA has on hair cycle induction (50, 51). Some study has use CsA to induce the hair growth in a small region. The hair cycle then spread outwards and performs a propagation manner (24).

1.4 Introduction of sympathetic nerve (SN)

The sympathetic nerve is a division of the autonomic nervous system. It releases norepinephrine to activate the target organs which express adrenoceptor to manifest the fight-or-flight response. The serious reaction, such as pupil dilation, increase heart rate, slow gut motility, hair erection, etc., activates. However, the stress hormone, norepinephrine (NE), has been unveiled that it modulates the physiological effect on several tissues, including the metabolism of all CNS cells in brain (63), rescuing acetaminophen-induced injury in liver (64-66), mediating the epithelial wound repair and mucous production in lung (67, 68), recruiting and activating the immune system (69), differentiation of the stem cells (70-73), and melanogenesis (74). The different level of NE expression leads to different results, either proliferation or apoptosis, in the cardiac fibroblasts cells (75), and chondrocytes (76). It has been discovered NE can also regulate the keratinocytes regeneration (77-79) and is involved in hair growth (31).

doi:10.6342/NTU201701146

1.4.1 Structure and development

Structurally, sympathetic nerve (SN) can be divided into two kinds of neurons: pre-ganglion and post-ganglion neurons. The pre-ganglion neurons reside in the thoracolumbar region of the spinal cord and extend its axon to one of the paravertebral ganglia. It synapses with the post-ganglion neurons in the ganglion and secretes the acetylcholine to transmit the signal to the post-ganglion neurons. The post ganglion neurons extend its axon to the target organs and tissues.

In the development, sympathetic nerves are derived from the trunk neural crest cells. These cells proliferate and differentiate into the mature sympathetic nerve(SN) (80). In mouse, the SN begins to extend at E12.5 along the motor efferent and sensory afferent axons which develop at E9 and E10 respectively. The past study discovered that the both sensory and motor axons are necessary for the proper SN development. The extended SN climb to the skin at the specific site and then spread its axons in the skin (81). In the rat skin, the tracks of compact SN endings are arranged into several loops (82) (Figure1.5).

doi:10.6342/NTU201701146

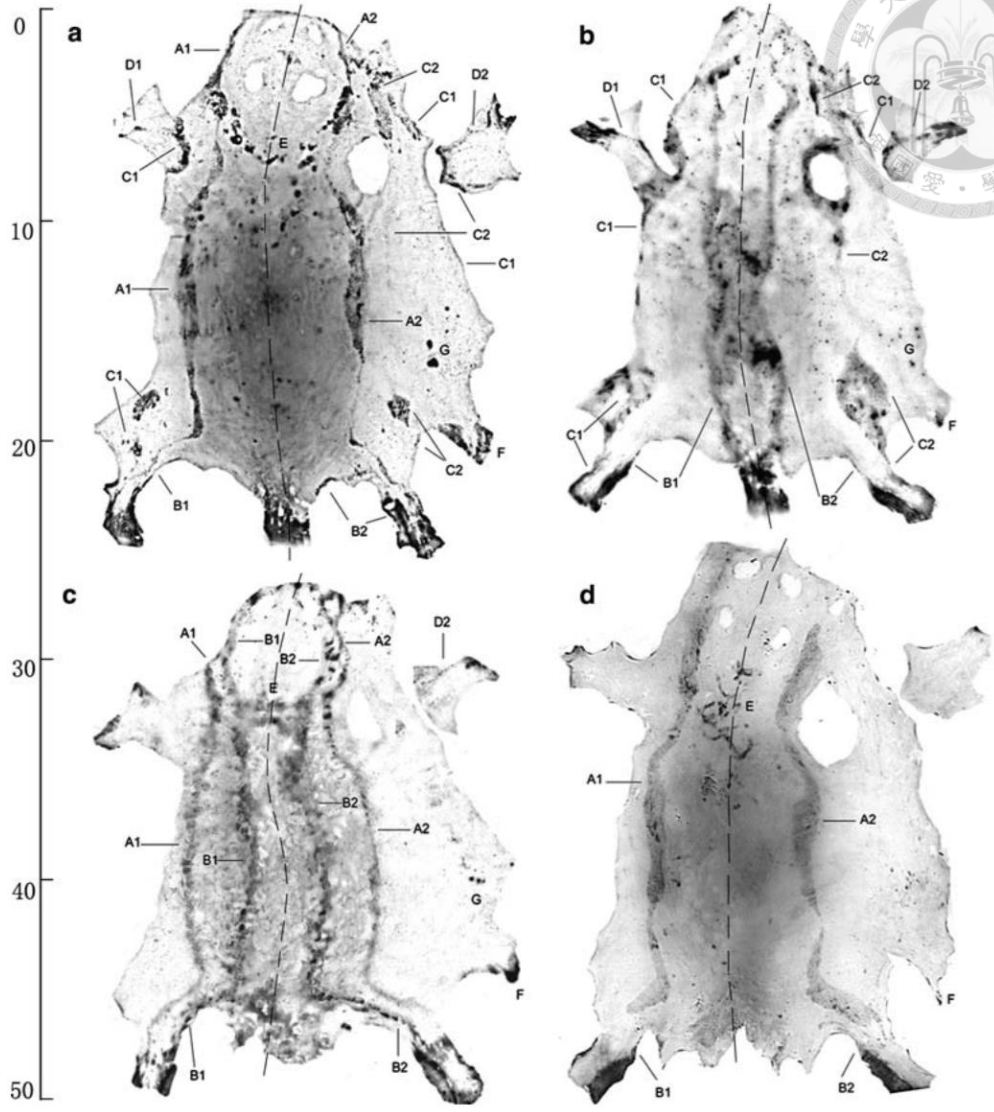

Figure 1.5 Autoradiograms of the whole rat skin to show the sympathetic nerve linear distribution (82)

1.4.2 Role in wound healing

The effect of norepinephrine (NE) on cell proliferation and differentiation has displayed on the keratinocytes as well(83, 84). During wound healing, the NE impedes the cell migration into the wounding area, slows down the cell proliferation and stimulates cell differentiation(83, 85, 86). Except for the SN itself who is the prime supplier for NE, keratinocytes were discovered to self-produce certain amount of

doi:10.6342/NTU201701146

NE(77, 84). However, the purpose of the ability to secrete NE in keratinocytes is still unclear.

1.4.3 G-protein transduction pathway

NE induces the activates beta-adrenoceptors(BARs). The classical pathway of the BAR, G-protein receptor, is through cAMP (86, 87) (Figure 1.6). Even previous studies have indicated the ERK may be down-regulated by the PP2A after B2AR agonist addition, B2AR has been investigated the activation of the ERK signaling pathway in rat and mouse cardiomyocytes after treated with the isoproterenol (88-92). Wenwu Li demonstrated the increase of p-ERK/p-MAPK expression keratinocytes cultured with NE (93). In another study, it was shown that B2AR agonist enhances the Wnt signaling through phosphorylating the beta-catenin to prevent it from ubiquitination in the alveolar epithelial cells (94). B2AR activation promotes the cell differentiation through PKA activation which results in the intracellular calcium concentration change (77). Increased level of calcium in keratinocytes inhibited the proliferation and induced the differentiation (95, 96).

doi:10.6342/NTU201701146

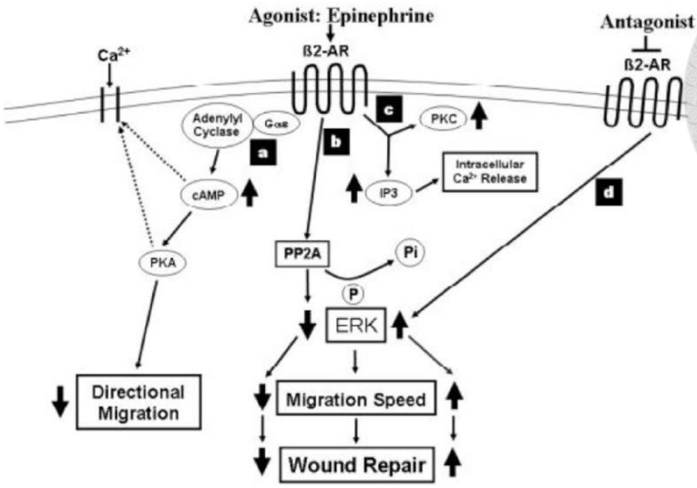

Figure 1.6 B2AR transduction pathway (86)

doi:10.6342/NTU201701146

1.5 Relationship between SN and hair cycle

In the past clinical study, having the beta-2-adrenoceptor (B2AR) antagonist leads to alopecia (36). This phenomenon shed insight on the relationship between hair growth and NE. Hair is a complex structure which is highly innervated with the sympathetic neuron. The amount of the SN fiber displays an oscillation through the hair cycle (31). It is suggested that the SN fibers grow to the maximum number in the middle phase of the anagen. On the other side, a clump of cells in bulge strongly expresses B2AR at anagen II during the hair cycle (31). This neuro-hair follicle interaction reveals the potential involvement of NE in the hair growth.

It has been unveiled that the depletion of SN, either surgical denervation or chemical sympathectomy, affects the hair growth(37, 40). Both approaches indicated the disruption of hair growth after the denervation. The effect of SN on hair growth has been studied. Back to 1958, Syoiti Kobayasi has operated a surgical denervation experiment on the dog. He cut at different site of the nerve trunk, including the cutaneous nerve, anterior and posterior spinal roots, and branches of thoracic SN. In the truncation of the SN experiment, the hair grew in a slower rate. And two dogs showed no hair growth after the operation (37). However, Marcus Maurer has considered that nerve innervation has no influence on anagen development (97). He conducted the unilateral surgical denervation to test the effect of SN depletion on different hair growth conditions, including spontaneous entry, CsA-induced, and depilation-induced. The results revealed the slight difference of slower growth rate in the depilation-induced anagen development. However, it showed no difference in the other two anagen induction measures. These contradicting results might be contributed by the use of the different animal model or different denervation site. According to Syoiti Kobayasi,

doi:10.6342/NTU201701146

different animals showed the different pattern of hair growth after surgical nerve truncation (37). Like sympathectomy demonstrated no effect on the cat. Moreover, the denervation site might also affect the outcomes. Cervical denervation in dogs accelerated the head hair growth, while thoracolumbar denervation retarded the hair growth of the hind limb (37).

The further experiments were operated in the specific SN depletion manner with 6-hydroxydopamine (6-OHDA) without sensory nerve devastation. 6-OHDA which destroyed SN specifically was originally used to mimic the Parkinson's disease module in mice (98). It was up-taken by the dopamine transporter (DAT) responsible for clean-up of redundant SN in the synapse. It causes the oxidative stress and leads to cell apoptosis in the cell through the blockage of mitochondrial activity(98). Hence, 6-OHDA was considered as a safe drug with its high specificity, and it was used in the SN depletion in later studies (98). Mari Asada-Kubota investigated the SN function in hair morphogenesis (38). After subcutaneously chemical sympathectomy, the SN depletion area was performed a slower development compared to the untreated area. It was believed that SN has an impact on the hair growth (38). 6-week-old mice had a significantly slower rate after SN depletion with 6-OHDA (39). Furthermore, evidence shows that AR-agonist, isoproterenol(ISO), accelerates the hair growth at anagen III to anagen IV (40). Hence, the increment of SN fibers was thought to facilitate the hair follicle elongation. Without the SN, the growth of hair follicles will be slowed down or even interrupted.

doi:10.6342/NTU201701146

1.6 Motivation

Hair cycle exhibits a particular pattern. In rat, the begin of hair cycle starts at two sides of the body and then propagates up to the middle of the back (99). The dissection of the early growing out hair region, lateral sides, tissues exhibits denser SN fibers in rat (82). It raises the question that if SN plays a crucial role in hair cycle entry and if SN is the liaison of each hair follicles on hair cycle synchronization. In our pilot study, we demonstrated that, with early treatment, hair growth of the SN-depletion area was unsynchronized with the whole body. The telogen-anagen transition was interrupted when SN was depleted at telogen. It took about four days to reach the full anagen SN depletion at early anagen (Figure 1.7). It was a surprise that hair cycle was interrupted with a pure depletion of SN while so many factors control it. Hence, we hypothesized that the function of SN serves as a guard who maintain the niche at a higher resting potential for early anagen entry. In my thesis, I will try to address the role of sympathetic nerves in hair regeneration and to identify the cellular and molecular mechanism to explain how sympathetic innervation affect hair cycle.

doi:10.6342/NTU201701146

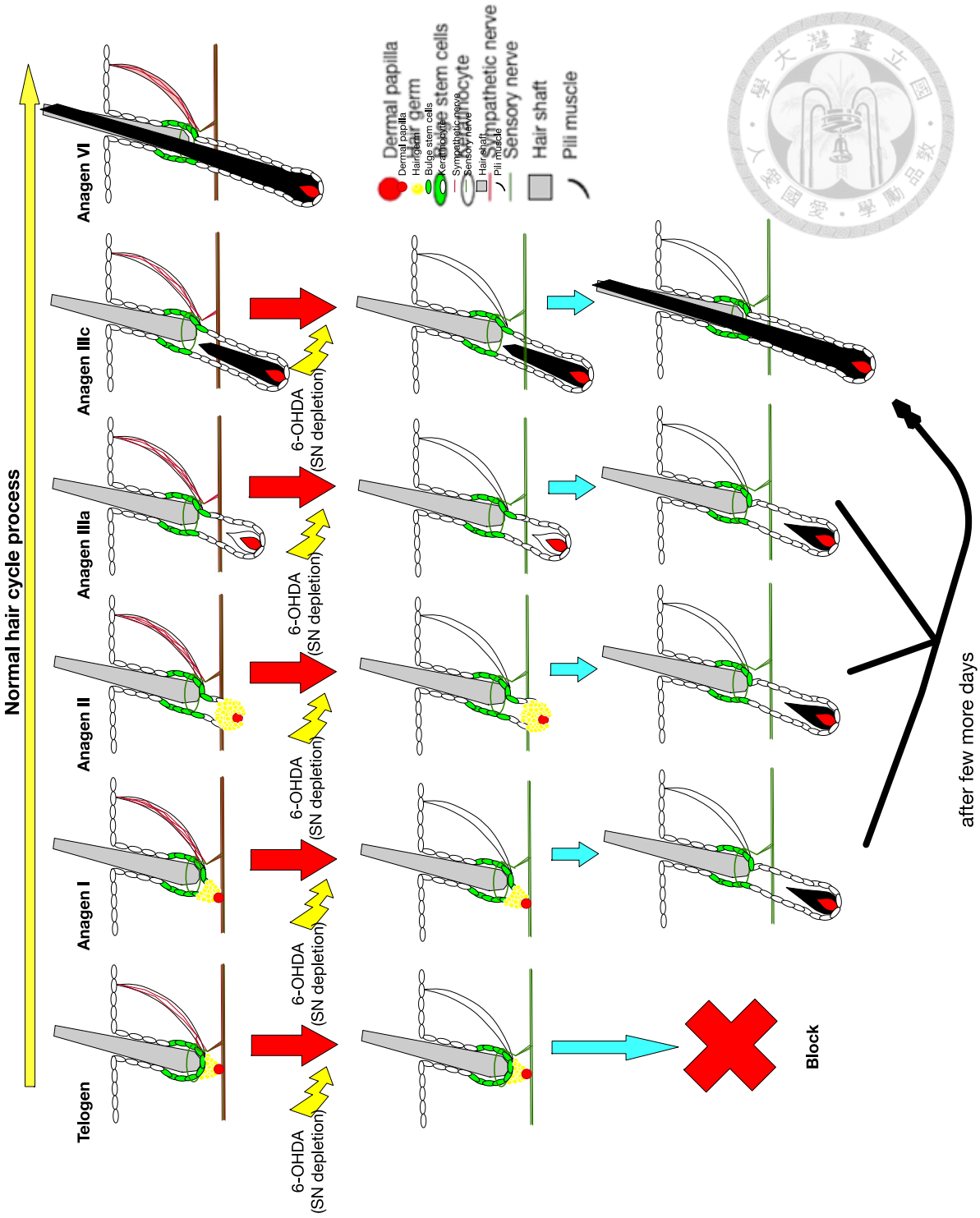

Figure 1.7 The effect of SN depletion on hair growth

doi:10.6342/NTU201701146

1.7 Specific Aim

To understand the role of the SN on hair growth. First, we will characterize the cell dynamics in sympathetic innervation and hair cycle in hair cycle in mice. Second, we will confirm the cellular relationship between sympathetic nerve and hair follicle stem/progenitor cells through sympathectomy during hair cycle. Third, the molecular mechanism will be identified by analyzing the qPCR data, and confirmed by small chemical drug or artificial neurotransmitter.

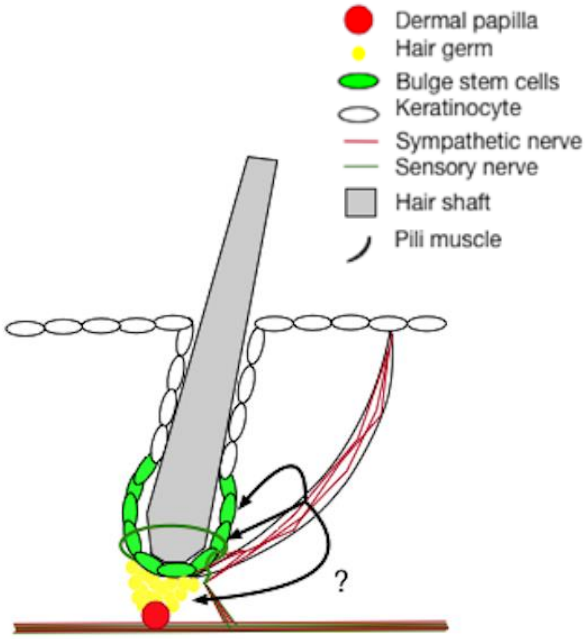

Figure 1.8 Question on how SN affect hair growth

doi:10.6342/NTU201701146

Chapter 2 Materials and Methods

2.1 Mice

C57BL/6 mice were obtained from the National Laboratory Animal Center (NLAC). All animal experiments were approved by NTU Institutional Animal Care and Use Committee (IACUC). All mice were anesthetized by 30μl anesthetizer, which was made by 5ml Zoletil® (Vibrac, FR) dissolved in 6.25ml saline and 1.25ml Rompun® (Bayer, German). To check the stage of hair cycle, dorsal skin hair was shaved off by the electric razor at two days before the experiments. Cervical dislocation in anesthetic condition was conducted at the end of the experiments.

2.2 Neuro-pharmacological manipulation

2.2.1 Chemical sympathectomy (6-OHDA)

Shaved mice had the 6-hydroxydopamine (6-OHDA) subcutaneous injection in the right-lateral region. The 3g/l 6-OHDA was prepared in saline (0.9% NaCl), at the volume of 100μl, in 3 week old mice, and 200μl, in 7 week old mice. The control group was injected with same volume saline only. The 6-OHDA injection was applied once on either P23, P25, P27, P29, or P47, depends on the purpose of the experiment.

2.2.2 Beta-2-adrenoceptor induction (isoproterenol)

Isoproterenol (ISO) (1g/l) (SIGMA, USA) was dissolved in the saline. After mixing 200μl of ISO with 0.25g hand cream (Neutrogena, Korea), the mixture of ISO was topically applied on the shaved back skin for seven consecutive days. The mice were anesthetized while the topical application.

doi:10.6342/NTU201701146

2.3 Hair cycle induction

2.3.1 Physical hair cycle induction (waxing)

Wax strip (VIGILL, TW) was used during the telogen of the hair cycle. Hand temperature was raised to melt the wax under rubbing the wax strip. The strip was pasted onto the shaved back. The wax strip was left on the skin till solidification. Then, the wax strip was stripped out to remove the hair roots.

2.3.2 Chemical hair cycle induction (CsA)

After the anesthetization, the mouse was applied with the volume of 7μl cyclosporine A (TOCRIS, UK), dissolved in 75% alcohol, onto the upper-middle region of the back for 10 consecutive days. The size of the applying area was a 1.5mm x 0.5 mm square. Hair cycle was induced by the CsA in the applying region and propagated the hair wave down to the bottom of the back.

2.4 Skin harvesting

The skin was harvested at the end of each independent experiments. First, all mice were anesthetized and sacrificed under the cervical dislocation. Then, scissors and forceps were used to cut and move the skin onto the weighing paper. The samples were immersed in the 4% paraformaldehyde (81) (Bio Basic Inc., Canada) for overnight. Next day, the skin was moved to the 75% alcohol to store, and further processes for morphometric analyses were described below.

2.5 Cryosection

The skin samples were washed with phosphate buffered saline (PBS) and were dehydrated with sequential replacement of 50%, 75%, 95%, 99% ethanol for 5 minutes

doi:10.6342/NTU201701146

at each step to remove lipid droplet in the dermis layer. The treated skins were replaced with 95%, 75%, 50%, and d_2H_2O for 5 minutes at each step. The treated skin, then, was embedded in OCT (Sakura Finetek USA) at -20°C for cryosection. Back skin samples were cut into 100μm thick in the cryostat at −20°C and put into 1.5 mL eppendorf tubes with PBS to remove OCT

2.6 Immunofluorescence staining

2.6.1 100μm samples immunofluorescent staining

For 100μm samples immunofluorescent staining, the section skins were incubated with blocking reagent 5% bovine serum albumin (BSA) for half hours and switched to staining reagent (blocking reagent, 1st antibody) for overnight at 4°C with a gentle shake (40rpm). The section skin samples were washed with 200μl phosphate buffered saline with Tween 20 (PBST) (PBS, 1% Tween 20) for half hour three times at room temperature and incubated with the secondary antibody with DAPI (1:1000) for immunofluorescence and nuclear staining. The dilution of primary antibodies was listed in Table 1. After 24 hours, the skin samples were washed with 200 μl PBST for half hour three times at room temperature and mounted on cover slides with fluorescence mounting medium (Dako). The images acquisition was using Zeiss LSM880 confocal microscopy system, and the z section was 1μm. For 3D imaging reconstruction, the confocal images were analyzed with Avizo software.

doi:10.6342/NTU201701146

2.6.2 Whole skin IHC staining

For whole skin staining, the section skins were incubated with blocking reagent 5% BSA for 2 hours and switched to staining reagent (blocking reagent, 1st antibody) for overnight at 4°C with a gentle shake (40rpm). The section skin samples were washed with 1mL PBST for an hour three times at room temperature and incubated with the secondary antibody with DAPI for immunofluorescence staining and nuclear labeling. The primary antibodies were used at following dilutions, dissolved in 5% BSA. After 7 days, the skin samples were washed with 1 mL PBST for an hour three times at room temperature, incubated in 1ml benzyl alcohol benzyl benzoate (BABB) (1:2 of benzyl alcohol (SIGMA, USA) and benzyl benzoate (SIGMA, USA)). Finally, the samples were mounted on cover slides with BABB. The samples were endured to be flattened. The images acquisition was using Zeiss LSM880 confocal microscopy system, and the z section was 1μm. For 3D imaging reconstruction, the confocal images were analyzed with Avizo software.

Primary Antibody				
Product Name	**Host of Ab**	**Dilution Ratio**	**Purpose**	**Brand (catalog number)**
Anti-Tyrosine hydroxylase	Sheep	1:200	Staining for sympathetic nerve	Minipore
Anti-Beta2-adrenoceptor	Rabbit	1:100	Staining for B2AR	Alomone labs
Anti-Ki67	Rabbit	1:300	Staining for proliferation cells	Thermo
Anti-Cytokeratin 15	mouse	1:100	Staining for bulge stem cells	Thermo
Anti-Calcitonin gene-related peptide (CGRP)	Rabbit	1:300	Staining for sensory nerve	Cell Technology Signaling
Secondary Antibody				

doi:10.6342/NTU201701146

Product Name	Dilution Ratio	Brand (catalog number)
Alexa Fluor® Cy3 AffiniPure Donkey Anti-Sheep IgG (H+L)	1:400	Jackson ImmunoResearch (713-165-147)
Alexa Fluor® Cy3 AffiniPure Donkey Anti-Rabbit IgG (H+L)	1:400	Jackson ImmunoResearch (712-165-152)
Alexa Fluor® 488 AffiniPure Donkey Anti-Rabbit IgG (H+L)	1:400	Jackson ImmunoResearch (711-545-152)
Alexa Fluor® 488 AffiniPure Donkey Anti-Mouse IgG (H+L)	1:400	Jackson ImmunoResearch (715-545-151)
Alexa Fluor® 647 AffiniPure Donkey Anti-Rabbit IgG (H+L)	1:400	Jackson ImmunoResearch

Table 1 Primary and Secondary primers lists used in immunofluorescent staining

2.7 Cell sorting

2.7.1 Sample preparation

The whole back skin was isolated from the fascia by the scissor after wiping with alcohol cotton sheet. The pins were used to stretch, flatten and fix the skin onto the Styrofoam lid with the subcutaneous facing upward. The lipid layer was gently scratched out by the scalpel. Then, the skin was turned over and paved on the culture dish, wash with 10ml PBS and the skin were digested with 10ml 0.25% trypsin-EDTA in a 37oC incubator for 30 mins. The skin must be endured to be flattened and free floating.

doi:10.6342/NTU201701146

2.7.2 Keratinocytes isolation

The following steps were performed on the ice. After the digestion, a forceps and scalpel were used to scrape all the hair off the skin, in the direction from anterior to posterior. Since the hair follicles tend to form clumps, the skin was tempted to scrape in a small area at a time. The hairless skin was, then, transfer to the other dish with 10ml PBS. The remain hair follicles on the scraped skin were scraped off into the PBS. The clumps of hair follicles were broken down by the forceps and scalpel into single hair follicles. The mixture of hair follicles and medium, trypsin or PBS, was vigorously triturated by using a 10ml pipette for 10~20 times to break down all clumps. The hair follicles suspension was transferred to the 50ml centrifuge tube. The dish was rinsed with 10 ml PBS and transferred to the same tube. The suspension was filtrated through the 70μm and then 40 μm cell strainers into the other 50ml centrifuge tubes. The origin tube was washed with the PBS and filtrated through the cell strainers till the last tube reached 50ml. The suspension was centrifuged for 15mins under 300g at 4oC. The supernatant was removed, and the cell pellet was resuspended in 5ml staining buffer, which contained 3% FBS in PBS. The suspension was the centrifuged again for 5 mins under 300g at 4oC. The supernatant was removed, and the cell pellet was resuspended in 0.2ml staining buffer.

2.7.3 Cell staining

25μl of the control sample was aspirated into 5 FACS tube for single stain and un-stain use. The rest and suspension of test samples were moved to the FACS tubes as well. All samples were added with staining buffer to the volume of 0.2ml. The antibodies were in the dilution describing below: anti-Sca-1 (1:100) (eBioscience, US),

doi:10.6342/NTU201701146

anti-CD34 (1:100) (eBioscience, US), anti-CD200 (1:50) (eBioscience, US), and anti-integrin-a6 (1:300) (eBioscience, US). The samples were gently shaken and rest for 30 mins on ice. Follow up, each FACS tubes were added staining buffer to 4ml and centrifuged for 5mins under 300g at 4oC. The supernatant was sucked out, and 4ml staining buffer was added to resuspend the cell pellet. The process was repeated for 3 times. Finally, after the supernatant was sucked out, 500µl staining buffer was used to resuspend the cell pellet and filtrated through FACS strainer. The filtrated samples were added PI to stain the dead cells. The samples were stored on the ice and proceeded to the flow cytometry analysis.

The cells were sorted into FACS tubes containing 500µl of modification of Basal Medium Eagle (DMEM). The cells were centrifuged for 5mins under 300g at 4oC. The supernatant was aspirated and left around 7~10µl in FACS tubes. The samples were stock in the -80oC refrigerator

2.8 cDNA synthesis and amplification

The procedure followed REPLI-g® WTA Single Cell Handbook. Each sample with the volume of 7µl was placed into the micro-centrifuge tube and mixed with 4µl lysis buffer (Table 2). The tube was incubated at 24oC for 5min followed by 95oC for 3 min. After the sample was cooled to 4oC, 2µl gDNA wipeout buffer was added and the sample was heated to 42oC for 10 mins. Each sample was mixed with 7µl Quantiscript RT mix, mixture with 4µl RT/polymerase buffer, 1µl random primer, 1µl oligo dT primer, and 1µl Quantiscript RT enzyme mix. The mixture was incubated at 42oC for 60min followed by 95oC for 3min. The mixture was cooled to 4oC and 10µl ligation mix, with 8µl ligase buffer and 2µl ligase mix, was added. The mixture was incubated at

doi:10.6342/NTU201701146

24oC for 30min followed by 95oC for 3min. Finally, the 30µl REPLI-g SensiPhi amplification mix, containing with 29µl REPLI-g reaction buffer and 1µl REPLI-g SensiPhi DNA polymerase, was added into the mixture. The mixture was incubated at 30oC for 2 hours. The reaction was stopped by incubating at 65oC for 5 mins. The cDNA was stored in -20oC. The amplified cDNA was diluted 1:100 to be used in real-time quantitative polymerase chain reaction(RT-qPCR).

Lysis buffer		
Formula	**Final concentration**	**Volume (Total=200ml)**
5M NaCl	100mM	4ml
1M Tris (pH 8.0)	50mM	10ml
0.5M EDTA (pH 8.0)	50mM	20ml
10% SDS	1%	20ml
ddH_2O	-	146ml
20mg/ml Proteinase K	0.2 mg/ml	2ml

Table 2 The ingredients in Lysis buffer

2.9 Real time qPCR

The fluorescent substances, such as SYBR Green, embedded into the double strands DNA(dsDNA) increase under each PCR cycles. Real time-qPCR detects the variation of fluorescence intensity to quantify the amount of DNA was synthesized simultaneously. To complete the reaction, few substrates were prepared: 6.15µl of ddH2O, 0.3µl of forward primer, 0.3µl of backward primer (Table 3), 7.5µl of KAPA SYBR® FAST qPCR Master Mix, and 0.75µl of template cDNA (20ng/µl). All substrates were mixed

doi:10.6342/NTU201701146

into a micro-centrifuge tube. Each sample was prepared for 3 tubes, as n=3. The forward and backward primers used in the reaction were listed below.

doi:10.6342/NTU201701146

qPCR primer sequences		
Gene	**Forward primer (5' → 3')**	**Reverse primer (3' → 5')**
GAPDH	GGGAAGCCCATCACCATCT	CGGCCTCACCCCATTTG
B2AR	GTACTGTGCCTAGCCTTAGCGT	GGTTAGTGTCCTGTCAAGGAGG
Gli1	ATCACCTGTTGGGGATGCTGGAT	GGCGTGAATAGGACTTCCGACAG
Gli2	GTTCCAAGGCCTACTCTCGCCTG	CTTGAGCAGTGGAGCACGGACAT
ß-catenin	CGCAAGAGCAAGTAGCTGATATTG	CGGACCCTCTGAGCCCTAGT
Axin2	ACTGGGTCGCTTCTCTTGAA	CTCCCCACCTTGAATGAAGA
BMP4	TCCACTGGCTGATCACCTCAAC	AGTCCAGCTATAGGGAAGCAGTTTG

Table 3 Forward and reverse sequences used in the qPCR

All samples were moved into the 96-well and covered with a plastic membrane. After centrifuging, the well was placed into LightCycler® 96 Real-Time PCR system machine (Roche, Switzerland) for conduction the reaction and detection. The reaction underwent a cycle at 95ºC for 600 seconds. Then, 45 cycles at 95ºC for 10 seconds followed by 60ºC for 60 seconds were progressed. All relative genes expression level were analyzed by Excel (Microsoft), and the statistical analysis and diagram were perform by Prism 6 (Graphpad).

doi:10.6342/NTU201701146

Chapter 3 Results

3.1 Sympathetic nerves loop around hair follicle stem cells (HFSCs) and sympathetic nerve displays variation along the hair cycle

Sympathetic nerve fibers anatomically cling on the arrector pili muscle aside the hair follicles (100). The arrector pili muscles anchor one end at the epidermis and the other at the bulge region of the hair follicle. Sympathetic nerves originally grow along the sensory nerves to the bulge region and divert their endings to the arrector pili muscles while sensory nerves are encompassing around the bulge region of the hair follicles (11, 31). Due to the sympathetic nerves innervating closely to hair follicles, it has been suggested to participating in the hair cycle mediation. In this study, first of all, the sympathetic nerve was innervated around the secondary bulge area and showing a close association (Figure 3.1a). Furthermore, the SN innervated site is the region where HFSCs resides. The association of SN and hair follicle stem cells (HFSCs) showed no changes through the early to mid-anagen (Figure 3.1b). Meanwhile, at the telogen to anagen transition, the bottom of the bulge area began proliferating indicated by Ki67. After entry to the anagen II, $Ki67^{+}$ mainly exhibited at hair bulb. No Ki67 positive cell can be observed at the bulge at late anagen (Figure 3.1c). To understand if SN contributes to this phenomenon, its fiber was tracked through the hair cycle. The highest density of the SN fibers was observed in the anagen I. Anagen VI showed lowest density of SN fibers (Figure 3.1d).

doi:10.6342/NTU201701146

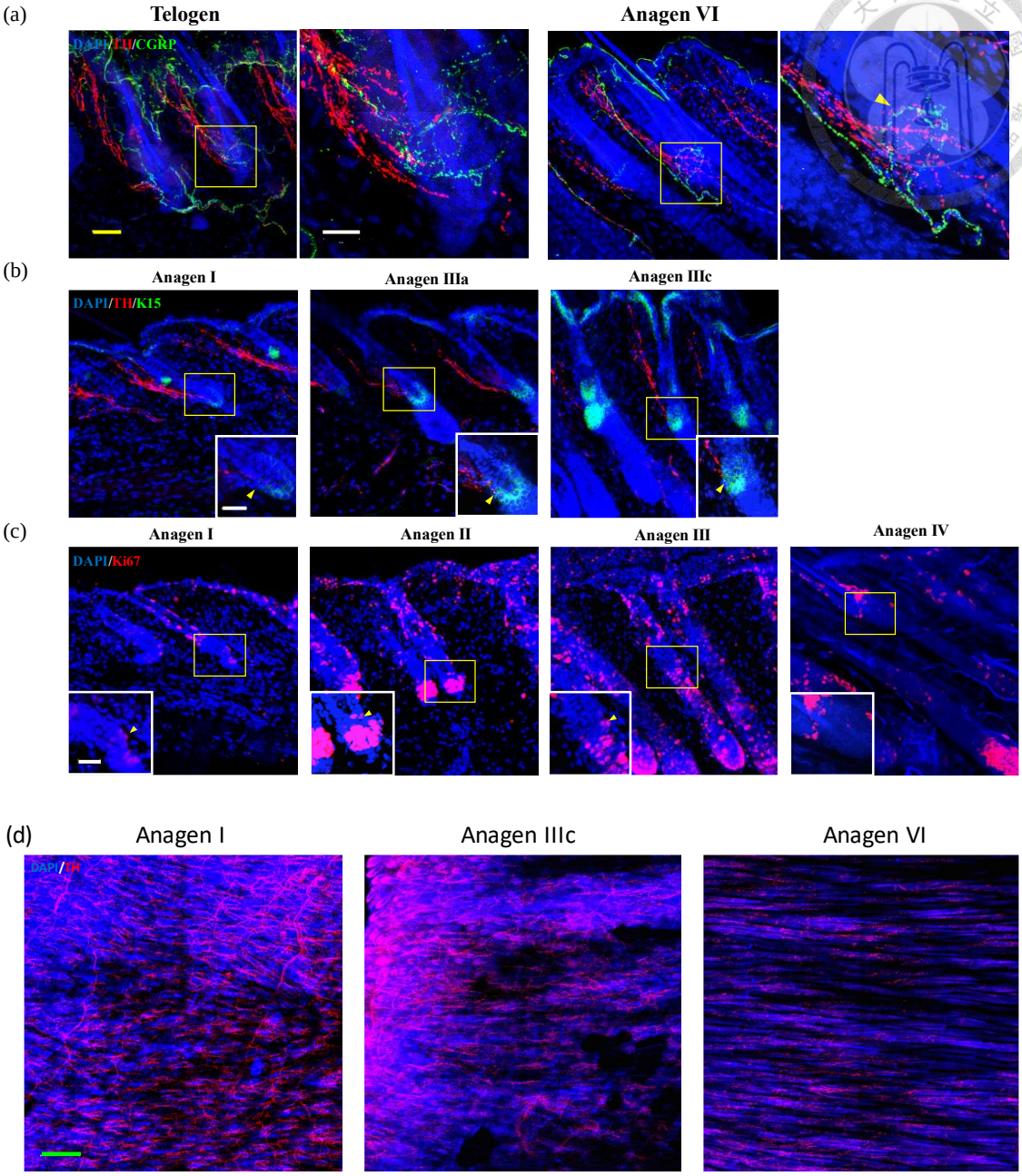

doi:10.6342/NTU201701146

Figure 3.1 SN innervated around HFSCs resident region and manifests variation along the hair cycle

(a) SN and sensory nerves innervate around the bulge was observed at telogen and late anagen.

(b) The sympathetic nerves associate with hair follicle stem cells which express K15. The sympathetic nerves association with $K15^+$ cells are hair cycle independent.

(c) The proliferation site was investigated through the hair cycle. Yellow arrow mark the expression of Ki67 at the bulge.

(d) The density variation of SN nerve fibers was studied through the hair cycle.

(White bar: 20μm, Yellow bar: 100 μm, Green bar: 200μm)

doi:10.6342/NTU201701146

3.2 Sympathetic denervation affects the hair cycle progression from telogen to anagen and anagen I to anagen III

In our data, the sympathetic nerve fibers oscillate with hair cycle (Fig 3.1d). We proposed that sympathetic nerves may be involved in hair cycle regulation. In previous study, the 6-hydroxydopamine (6-OHDA) treatment can efficient cause sympathectomy in mice model (40). Here, we try to address the role of SN in several hair cycle stages, including telogen to anagen, and early anagen to mide anagen. In the past study, 0.03mg/g bw 6-OHDA was the proper dosage for subcutaneous denervation. Higher than the concentration led to the skin erythema or, worse, ulcer (40). Here, the mice were subcutaneously injected with 0.03mg/g bw 6-OHDA dissolved in the volume of 200ul saline at the right side of the mice. The sympathectomy effect by 6-OHDA can extend to day 22 or even longer (Figure 3.2a). We cannot identify any SN neuron fibers (TH^+) in hair follicle after 22 days. Because the hair cycle stage correlate with skin color, we identify the skin color after sympathectomy. The sympathectomy regions did not show color change after two weeks, compared with saline treated region. Therefore, local administration of 6-OHDA at telogen could block telogen to early anagen entry (Figure 3.2b).

doi:10.6342/NTU201701146

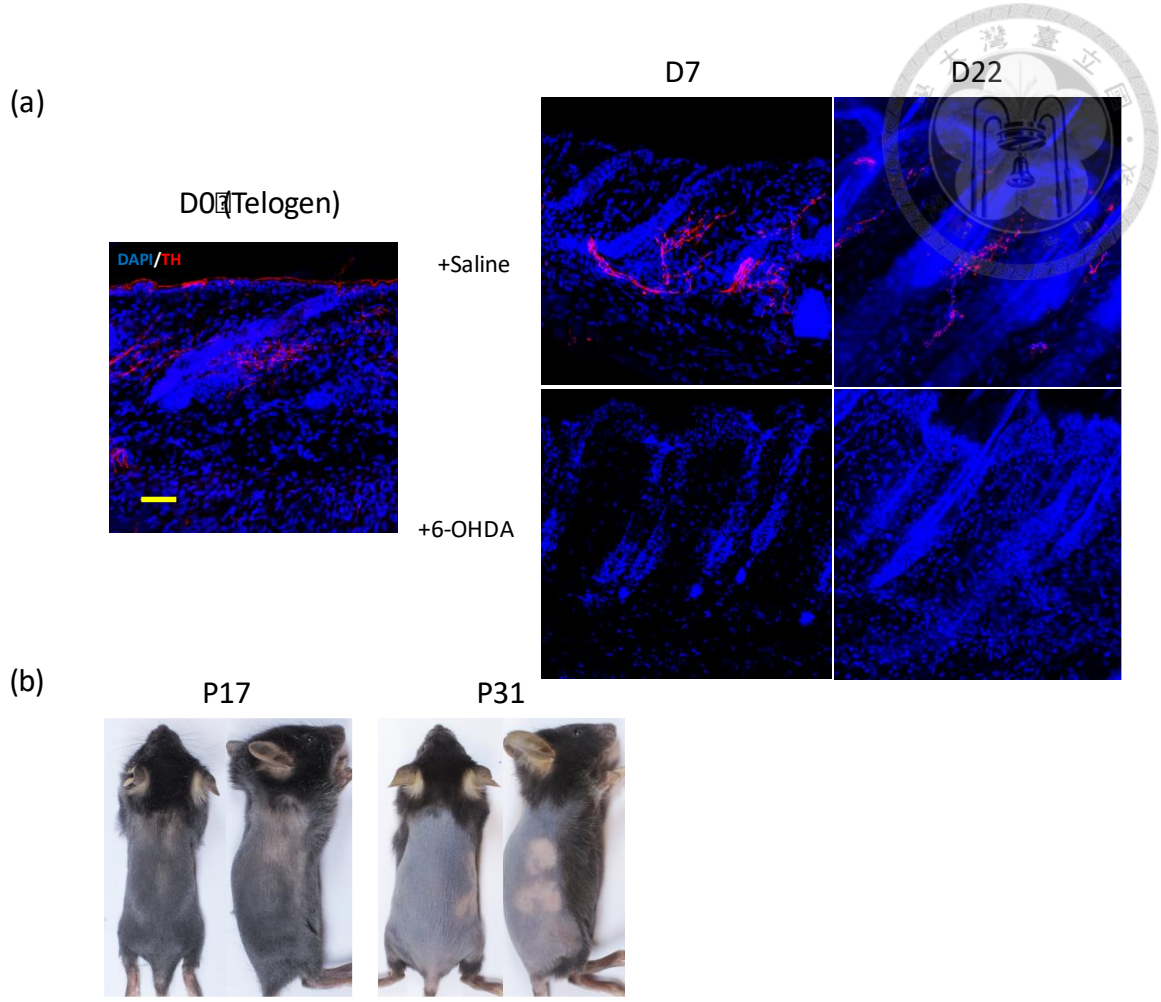

Figure 3.2 SN denervation affects the hair growth from telogen to anagen

(a) SN depletion was investigated after 6-OHDA administration at day 7 and day 22 (Yellow bar: 100 μm).

(b) The skin stayed in pink at the site of SN depletion by 6-OHDA at p17.

doi:10.6342/NTU201701146

The increment of sympathetic nerve fibers was indicated to happen at the middle stage of the anagen. The hair follicles also displayed the faster growth rate at anagen III in vitro after treating with the beta-agonist, isoproterenol (ISO) (31).

To further verify whether sympathetic nerves also promote the anagen I to full anagen transition, we perform denervation by local injection of 6-OHDA at individual hair cycle phase including P23 (telogen), P25 (anagen I), P27 (anagen II), P29 (anagen III), and P31 (full anagen) and identify hair cycle in progress till P38 (catagen). Intriguingly, local denervation can significantly delay hair cycle progress before P29 but did not show any effect on hair cycle phase after P29 (Figure 3.3a). The delay of cycle exhibited in the group with the SN depletion at P23, 27, 29; however, the SN depletion at P25 showed no unsynchronized effect in the administrated region. The phenomenon of the unsynchronized hair growth region at SN depletion site was considered as a slower hair cycle progress effect. The result was different from the blocking effect that exhibited in the former experiment when conducting the chemical sympathectomy at telogen (Figure 3.3b). Therefore, there should be other signals in promoting anagen progression, such as PDGFa (7). Here, we clarify that sympathetic nerves play important role in telogen to anagen transition and anagen I to anagen III progression.

doi:10.6342/NTU201701146

(a)

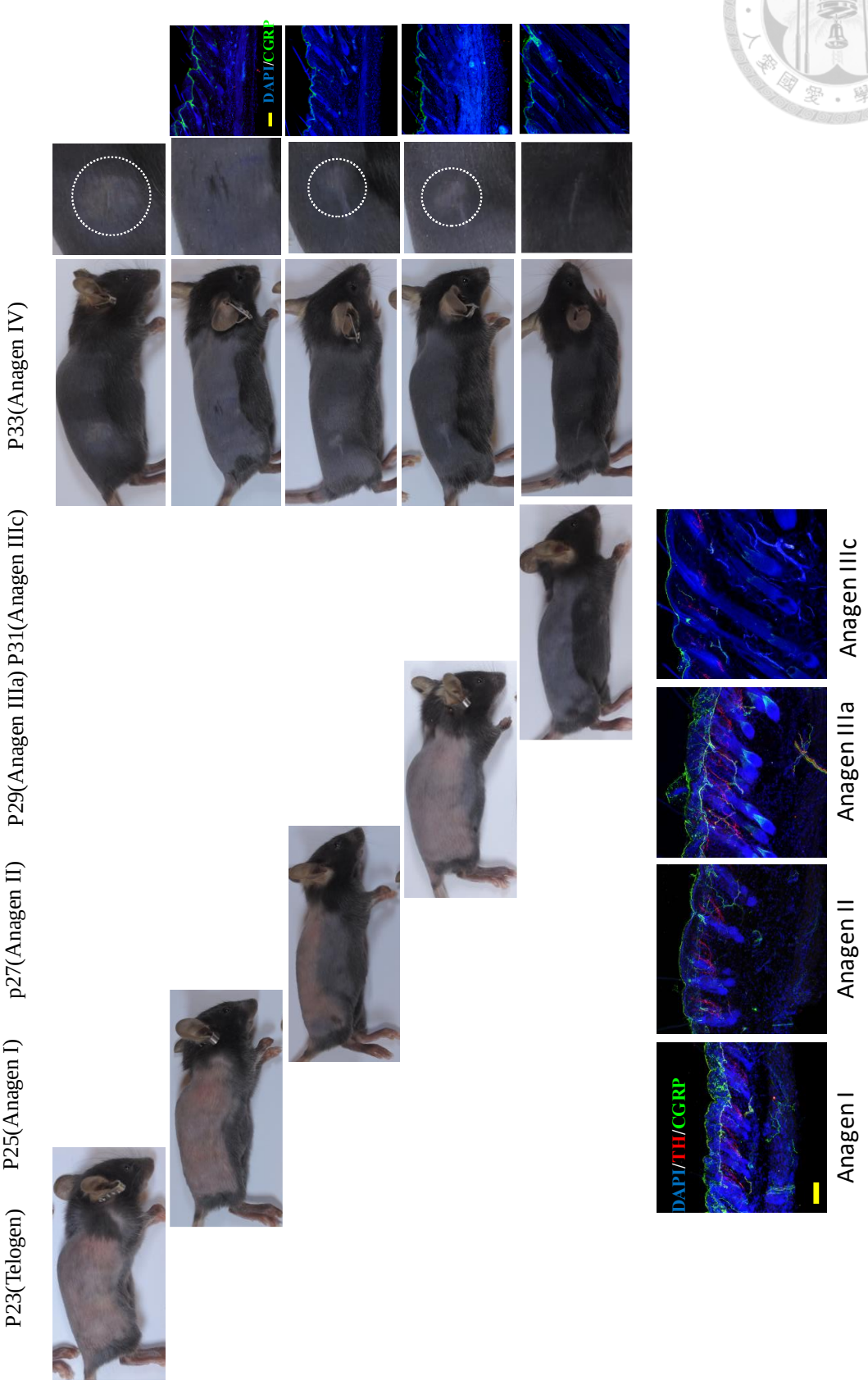

doi:10.6342/NTU201701146

(b)

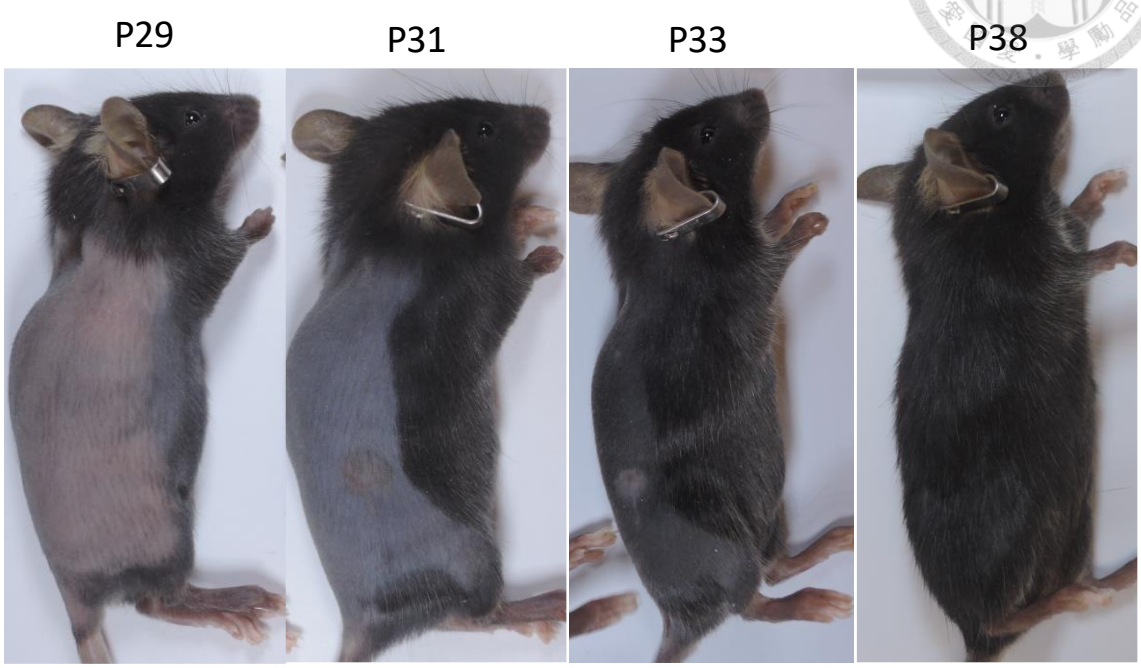

Figure 3.3 The effect of SN depletion at different stages of the hair cycle

(a) 6-OHDA was injected at different phases of the hair cycle. The mice were injected with 6-OHDA at the right side of the skin at P23, P25, P27, P29, P31. The correspondent hair follicle stages were anagen I, anagen II, anagen IIIa, anagen IIIc respectively. The delay of the hair cycle was discovered in the SN depletion area at P33. SN depletion at P27, P29 displayed the hair growth delay (white dash circle). No hair cycle was arrested at the mouse which was treated with 6-OHDA at P31. No SN expressed at P33 after SN depletion. (Yellow bar: 100μm)

(b) the further tracking of the hair growth at SN depletion site. All hair grew out at P38.

doi:10.6342/NTU201701146

3.3 Sympathetic nerve is required for hair wave progression

In the mice, the hair cycle initiate earlier in the lateral sides skin than the back skin. Importantly, the hair cycle entry exhibits a wave like process(101). The liaison of this process is still unclarified. SN depletion was shown to block and delay hair growth in the former studies. It was hypothesized if SN is responsible for the communication between follicles to undergo telogen-anagen transition. In previous study, CsA can promote early anagen entry. Here, we use CsA-induced hair cycle as a model to identify whether SN play an important role in hair wave generation. CsA was regional applied on the skin to create the hair wave. Volume of 20μl 2% CsA (dissolved in EtOH) was topically apply on the skin in a rectangle shape. After 9-days consecutive treatment, the rectangle area turned black. The hair wave can be observed at day 10~14. The black skin encompassed the lower right back area where SN has been depleted (Figure 3.4). Therefore, the SN is required for CsA induced hair wave transition.

doi:10.6342/NTU201701146

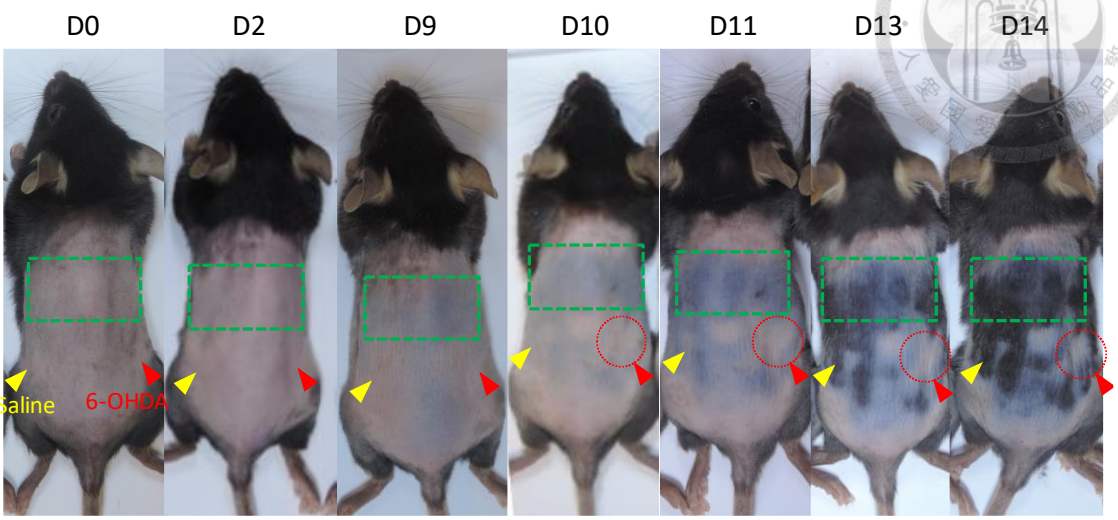

Figure 3.4 CsA-induced hair wave blocked by chemical SN denervation

Local effect of chemical denervation was investigated. Left side was injected with the vehicle, saline (yellow arrow). Right side was injected with 6-OHDA for SN denervation (red arrow). CsA was topically applied on the upper back skin close to neck (green square). The CsA-applied area turned black at day 9. The induced hair wave bypassed the 6-OHDA administrated area (red dash circle).

doi:10.6342/NTU201701146

3.4 Sympathetic nerve affects the hair growth through the beta2-adrenoceptor (B2AR)

To understand how SN mediates the hair growth. The target turned to the ideal target of SN, beta-adrenoceptors (BAR), which can be divided into three classes, beta-1, -2, -3 adrenoceptors (71, 102). BAR express in the epidermis, sebaceous glands, follicles, and blood vessels in the human skin (103). The B2AR is the only class of BAR that was investigated in the murine hair follicles (40). Therefore, it was suggested B2AR is the target that modulates the hair growth. The amount and distribution of B2AR were understudied. At anagen I, BAR was observed in the epidermis, sebaceous gland, isthmus, DP and the bulge. When entry the anagen IIIa, bulb expressed the high intensity of B2AR, and less B2AR was found in bulge area. Expression of B2ARat bulb plunged at anagen V. B2AR mainly displayed at the infundibulum, isthmus, epidermis, and adipocytes at anagen V (Figure 3.5a). It was discovered Ki67 displayed at the lower bulge and germ at the beginning of the anagen. Furthermore, Ki67 expressed mainly at the bulb and supra-bulb area at anagen IIIc (Figure 3.5a). The co-stain of B2AR and K15 demonstrated B2AR was overlapping with K15 at the bulge area at anagen I. With the progression of the hair cycle, B2AR expressed at the bottom of the K15-expressed bulge area at anagen IIIa. After the hair processed to anagen IIIc, only a few K15 positive stem cell at bulge still expressed the B2AR. The TH innervated at the keratinocytes that expressed both K15 and B2AR (Figure 3.5b). To test if expressed-B2AR plays a vital role in the hair growth regulation, BAR-agonist, isoproterenol(ISO) was topically applied to the skin. After consecutive 10 days of ISO topical application and rest till day 17, the hair grew out, The SN-depletion region shows no difference than the saline-administrated region (Figure 3.5c).

doi:10.6342/NTU201701146

(a)

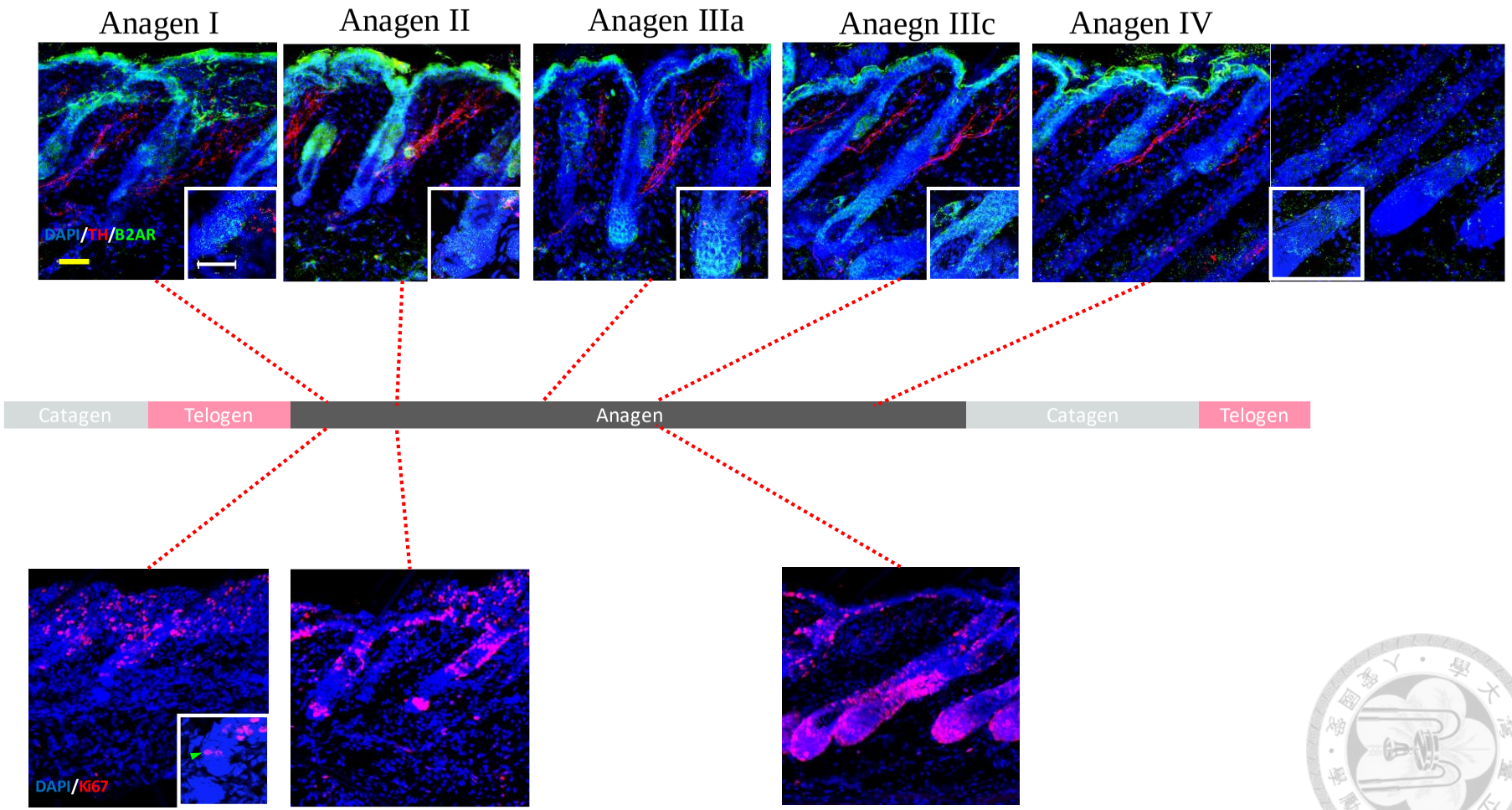

doi:10.6342/NTU201701146

(b)

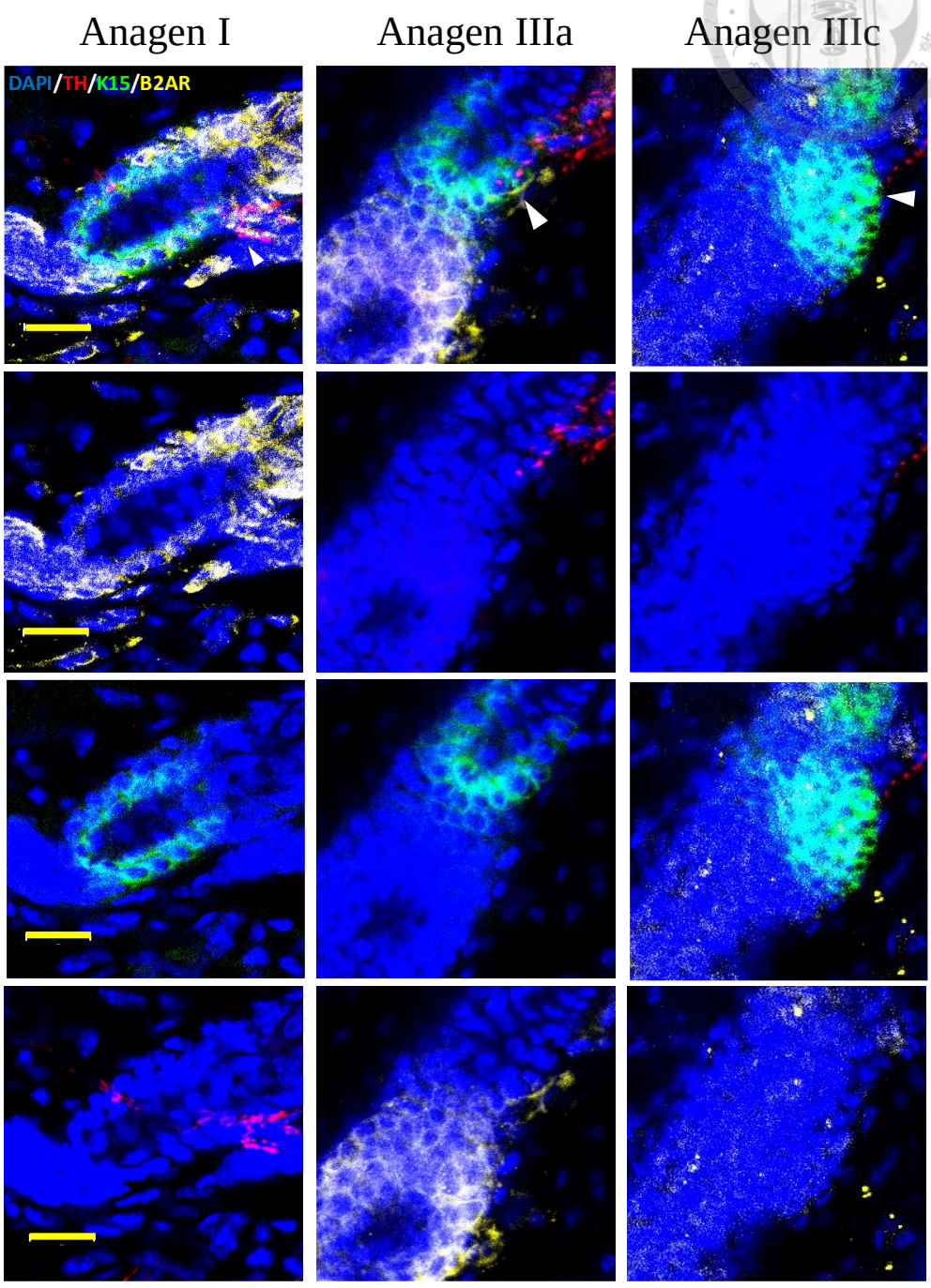

doi:10.6342/NTU201701146

(c)

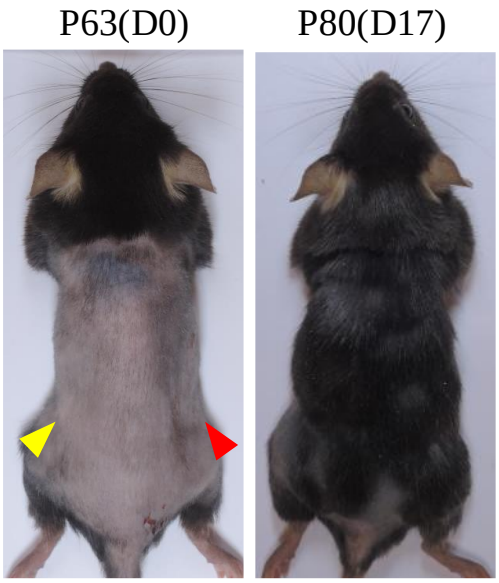

Figure 3.5 Sympathetic nerve affects the hair growth through the beta2-adrenoceptor(B2AR)

(a) Beta adrenoceptor expressed in the hair follicles through the hair cycle. Expression of the Ki67 at different phases of hair cycle. (Green arrow: expression of Ki67 at lower bulge) (Yellow bar: 20μm)

(b) Co-staining of K15, TH and B2AR at anagen I, anagen IIIa, anagen IIIc. (Yellow arrow: overlapping K15 and B2AR at bulge; Pink arrow: SN innervation site at bulge.) (Yellow bar: 20μm)

(c) ISO topical application on dorsal murine skin in inducing hair growth (Yellow arrow: saline administration; Red arrow: 6-OHDA administration)

doi:10.6342/NTU201701146

To identify the molecular mechanism by which SN facilitate cycle transition, we isolate bulge stem cells and hair germ stem cells from denervated or nondenervated skin and analyze the gene expression. bulge stem cells and germ stem cells were isolated from the p25-old mice who have been administrated with 6-OHDA on p23. The p23 mice were collected to investigate the signal variation in telogen-anagen transition. Bulge stem cells were gated with co-expression of CD34 and CD200. And germ cells were identified with CD200 expression only (Figure 3.6).

After RNA extraction and cDNA amplification process, we quantified the gene expression by real time qPCR. First, we check the genes expression including, *b2ar, gli1, gli2, wnt7b, ß-catenin, Axin2,* and *BMP4.*. B2AR was indicated to increase with the treatment of NE and decreased after differentiation (84, 93). B2AR were first candidates to be tested. In the result, B2AR expression in bulge showed no obvious difference from P23 to P25. However, after the depletion of the SN, The B2AR level raised significantly in the bulge. On the other side, SN depletion didn't show significant elevation of the B2AR expression level in germ. SN depletion showed no effect on the expression in germ (Figure 3.7).

Hedgehog pathway was the next candidate. In our unpublished data, the Hedgehog downstream signaling was activated after exposure the mice to the glittering light for a long duration. It was proposed to be related to SN which is the adrenergic control of stem cells migration in the circadian rhythm (69, 104). The level *gli1* and *gli2* performed no observable difference in telogen-anagen transition stage in bulge stem cells. But gli2 level raises at P25 control group in hair germ stem cells. SN depletion contributes to the decreased level of *gli1, gli2* signaling dominantly in bulge stem cells.

doi:10.6342/NTU201701146

Nevertheless, *gli1* level elevated and *gli2* level declined after the SN depletion in the secondary hair germ stem cells (Figure 3.8).

Next, catecholamine has been indicated to modulate the cell migration through *Wnt* signaling and regulate the lung epithelial cells activity through ß-catenin (58, 91). Hence, the downstream of *Wnt* has been examined. SN depletion contributed to the declination of *ß-catenin*, and *Axin2* in both bulge and secondary hair germ stem cells (Figure 3.9).

Finally, we examined the BMP4 at the bulge. After SN depletion, the hair cycle inhibiting factor BMP4 increase dramatically in the bulge stem cells. High BMP4 level can lead to the interruption of the hair growth (24). This data pointed out SN depletion can lower the BMP4 level and introduced the hair follicles back into a quiescent stage. Through gene expression analysis, we propose that sympathetic nerves can involve in mediating several signaling pathway, including, *bmp4*, *gli1*, *gli2*, *b-catenin* and *axin2,* that promotes hair follicle stem/progenitor cells activation and trigger the telogen to anagen transition (Figure3.10).

doi:10.6342/NTU201701146

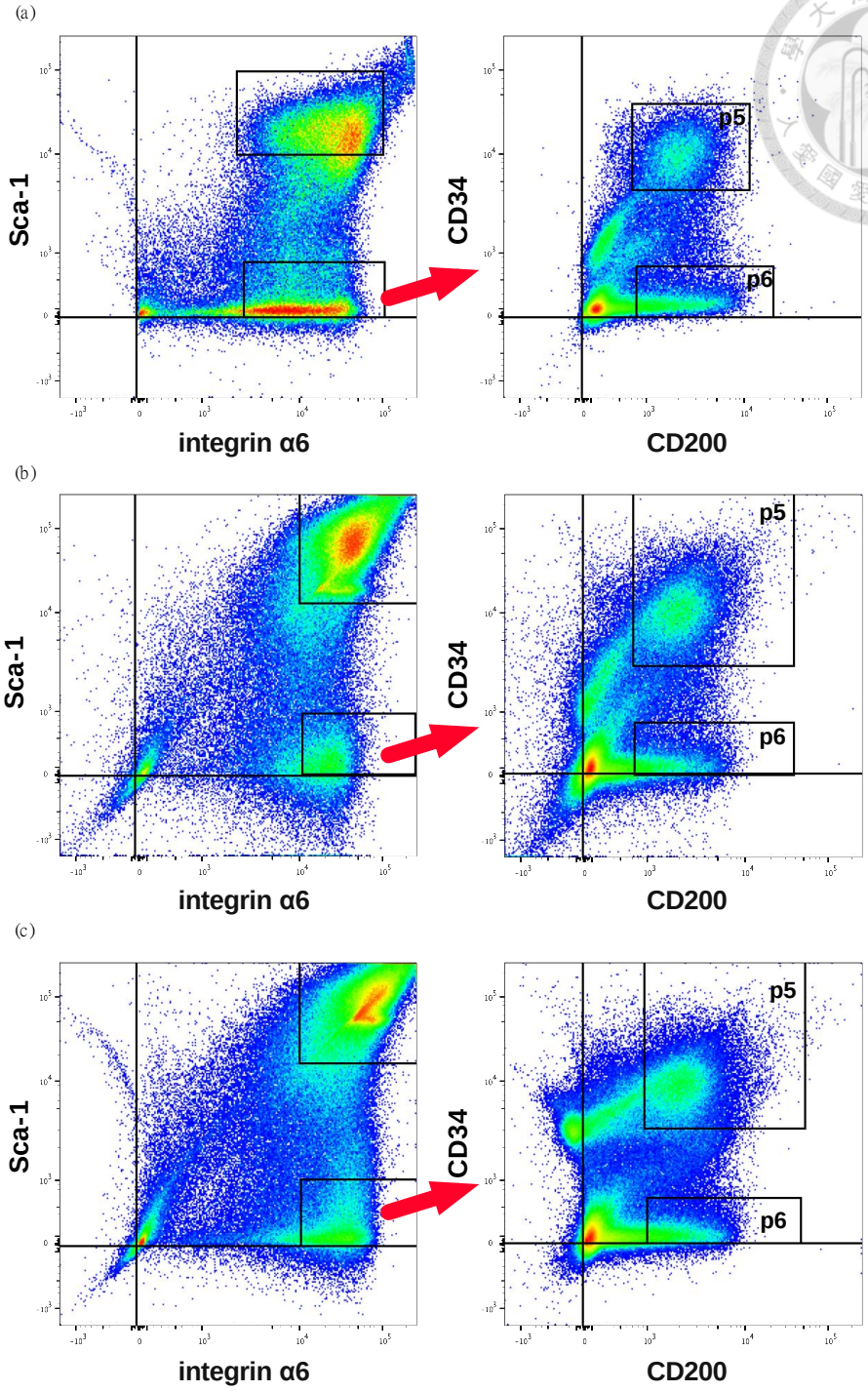

Figure 3.6 Cell sorting on p23, p25

Bulge and germ cells were isolated from the p23, p25(control), p25(SN-depleted) mice back skin. (a)P23; (b)P25(control) and (c)P25(SN)-depleted bulge: P5, germ: P6. (PE-Cy7: Sca-1; PE: integrin α6; APC: CD34; FITC: CD200)

(Bulge: Sca-1$^-$/ α6$^+$/CD34$^+$/CD200$^+$; germ: Sca-1$^-$/ α6$^+$/CD34$^-$/CD200$^+$)

doi:10.6342/NTU201701146

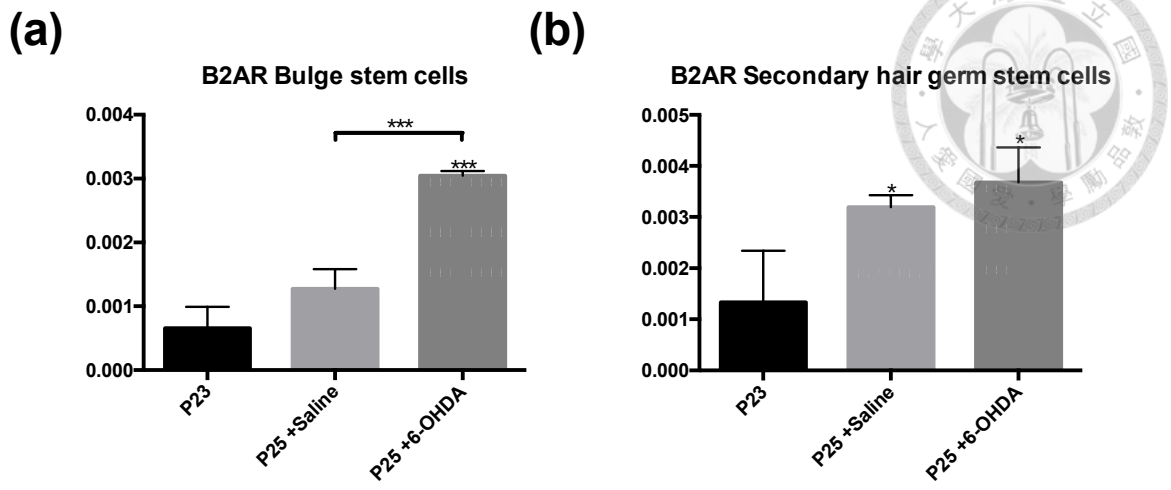

Figure 3.7 *B2AR* mRNA level at (a)bulge stem cells and (b)secondary hair germ stem cells: the effect of SN depletion (Normalized to GADH, n=3)

doi:10.6342/NTU201701146

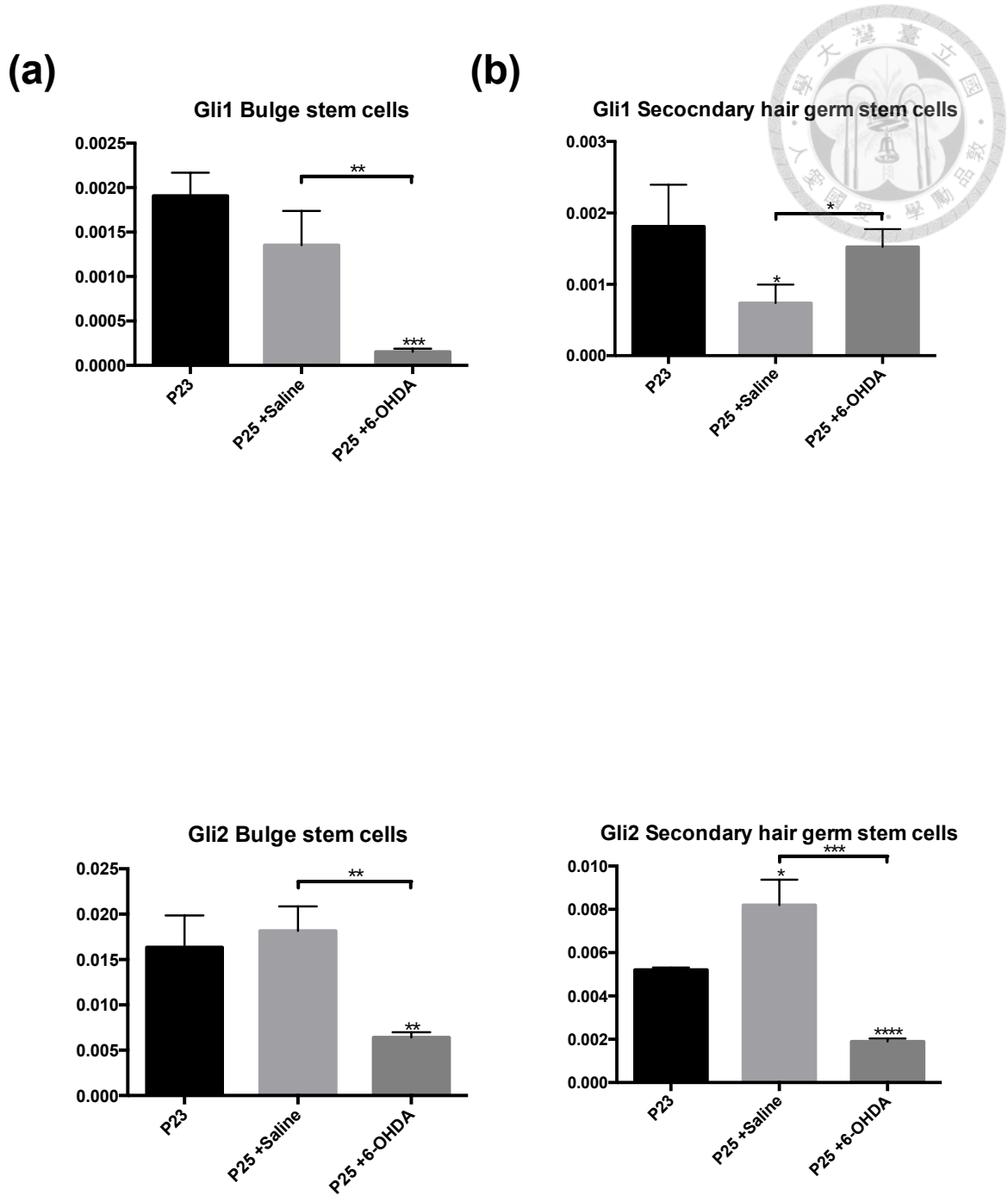

Figure 3.8 *gli1* and *gli2* mRNA level at (a)bulge stem cells and (b)secondary hair germ stem cells: the effect of SN depletion (Normalized to GADH, n=3)

doi:10.6342/NTU201701146

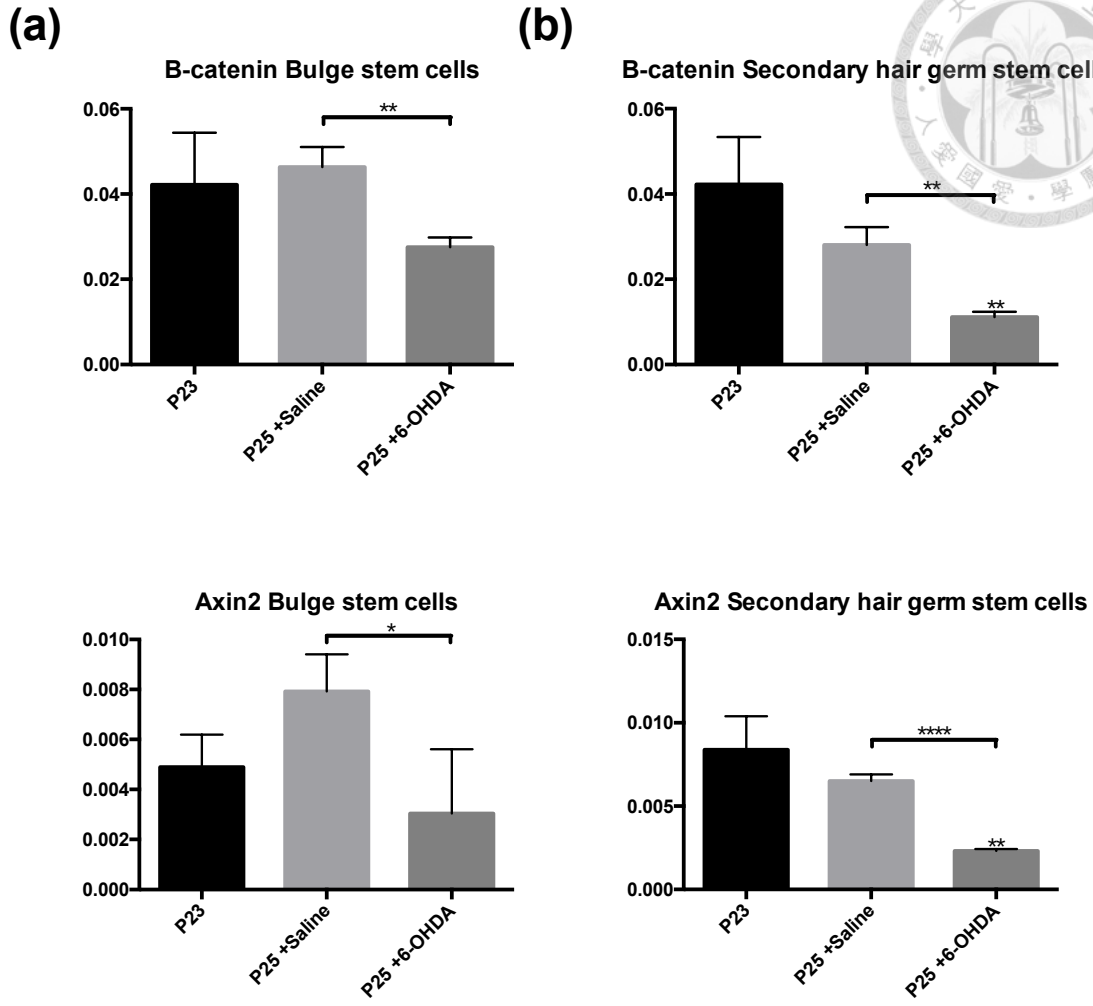

Figure 3.9 *b-catenin* and *axin2* mRNA level at (a)bulge stem cells and (b) secondary hair germ stem cells: the effect of SN depletion (Normalized to GADH, n=3)

doi:10.6342/NTU201701146

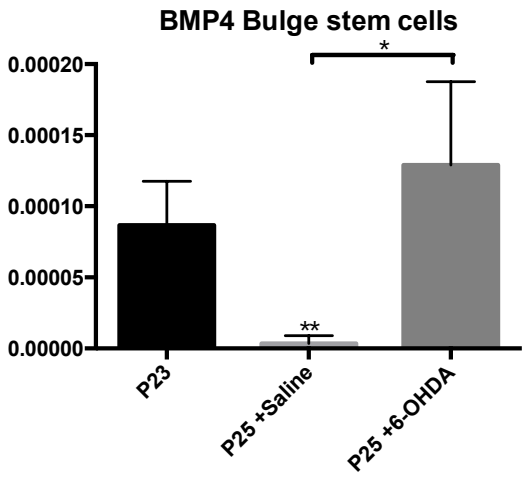

Figure 3.10 *bmp4* mRNA level at bulge stem cells (Normalized to GADH, n=3)

doi:10.6342/NTU201701146

3.5 sympathetic nerve not required for waxing-induced anagen entry

Hair plucking can stimulate an instant hair cycle entry (19). The cells in inner layer bulge express BMP6 and Fgf18 to suppress hair follicle stem/progenitor activation. Once the inner layer of hair bulge was ablated, the bulge stem cells are activated (9). In our study, we are wondering if SN involves in the depilation-induced hair cycle model. The mouse was subcutaneously injected the 3g/l 6-OHDA at the volume of 200μl at the lower back skin. After resting for 2 days, the back skin was waxed. The whole depilated site synchronously turns black on the 9th day after depilation. And no hair cycle delay or block was observed at the end of the experiment. As a result, the SN has no effect on depilation-induced hair growth (Figure 3.11).

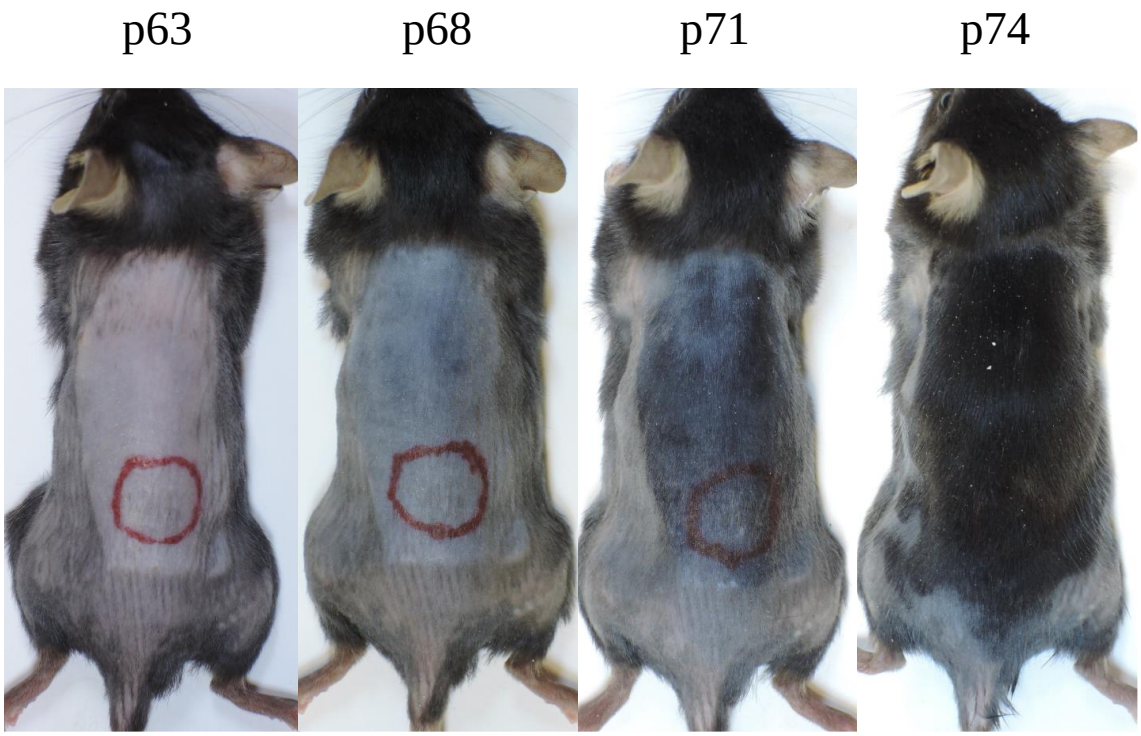

Figure 3.11 SN depletion has no effect on waxing-induced hair growth

6-OHDA was administrated at the lower back (red circle). The mouse was depilated at

doi:10.6342/NTU201701146

p63 and rested for 10 days. Skin turned black at the 5th day after depilation can be observed.

doi:10.6342/NTU201701146

Chapter 4 Discussion

In conclusion, the telogen-anagen trasition and early-anagen and mid-anagen progression of the hair cycle are under the adrenergic control. With the SN depletion at telogen or early anagen, the hair cycle was blocked, or the progression was slowed down, respectively. The phenomenon might be caused by the loss of the NE to maintain a transition threshold. In the anatomical data, the SN exhibited a close association with HFSCs at bulge. In the qPCR data, SN depletion at the telogen, level of BMP raised significantly. This indicates the hair follicle become more quiescent, harder to conduct the transition progress. SN was also indicated to regulate the hair follicle cells activity through affecting the hedgehog and Wnt/ß-catenin pathway. From the data, the SN was believed to establish the permissive niche which brings the cellular signals level close to activation threshold. After the telogen-anagen transition, the HFSCs has been activated. Simply depletion of SN decelerated the hair growth rate instead of arresting it in the certain stage when 6-OHDA is treated. Chemical sympathectomy at mid-anagen, blacken skin, had no effect on hair growth. This may be explained that, once the hair follicle has passed the transition threshold, the role of SN shifts. Combined with our TH and B2AR immunofluorescence staining, SN and B2AR highly expressed at early anagen. The density of SN decreased through the anagen. Expression of B2AR translocated from whole hair follicle downwards to bulb along the anagen progression. This explained why SN has some effect on cell proliferation at early anagen but not after mid-anagen. On the other hand, CsA and plucking were applied in the artificial-induced hair cycle model. SN depletion has shown the block of hair growth in CsA induced hair wave and has no effect on depilation-induced hair cycle.

SN has been studied about its effect on hair growth and keratinocytes proliferation and differentiation (31). However, no one has studied how SN affects the hair follicle

doi:10.6342/NTU201701146

stem cells, and which stages it plays the crucial role in the hair cycle. According to my result, the SN was suggested as a guard of telogen-anagen transition. Without it hair cycle will be blocked in a natural hair growth. It also affects the early anagen progression of hair follicle. Few signaling factors demonstrated the variation in the SN depletion condition. However, further research of SN effect on the surrounding cells is needed to investigate.

4.1 Relationship between SN and hair follicle

In the past studies, it had suggested that SN elongates its axon to the bulge area and migrates up to the epidermis along the arrector pili muscle (31). There is no evidence showing that SN endings have the direct connection with bulge keratinocytes. In my investigation, the close association between bulge and SN is exhibited at telogen and full anagen. SN projected its dendritic ending to the lower bulge area. This site had resided abundant of hair bulge ($K15^{+}$) stem cells. These cells are considered to be activated and are involved in the hair follicles elongation in the early anagen (105). Even it is not sure if it has a direct contact, it is close enough to affect the bulge with its secreting protein individually. These SN effect on the hair follicle is suggested to take place at the early anagen. At this stage, the overall density of SN fibers performed the highest in the skin among the density in later anagen stages which is consistent to the past study (31). Combined with the result of the expression of proliferation marker at early anagen at the SN projection site on bulge, it was hypothesized that SN participates in the early anagen development, but plays minor or no role in the late anagen growth. The hair follicles were discovered to grow at a faster rate from anagen III to anagen IV with the addition of BAR-agonist, ISO, in vitro (31, 39). In our early anagen SN depletion model, the growth rate was slowed down. This suggests the hair growth is

doi:10.6342/NTU201701146

control NE direct or indirectly.

Catecholamine was proved to affect the hair follicle and keratinocytes growth in vitro(39, 83, 85). ISO topical application on the mouse back skin has shown the early entry of hair cycle in this study. The induced hair growth also performed in the SN depletion site. This outcome confirmed phenotypically SN affects the hair growth through NE., the target of catecholamine, B2AR, was tracked through the hair cycle. The results have shown the expression of B2AR was almost exhibit in the whole hair follicle at the early anagen. The B2AR concentrated at the bulb area at the mid to late anagen. Then less intensity of B2AR was shown at the late anagen. The expression of the B2AR result was consistently similar to the Valker Steinkraus experiment which used the radioisotope to map the BAR in human skin (103). And the distribution pattern of the B2AR has also followed the Valdimir A. Botchkarev investigation. The B2AR translocate to the bulb area from the bulge site at late anagen (31). While the difference is, in the investigation, B2AR has expressed in the epidermis, isthmus and infundibulum region through the whole cycle. This study also demonstrated the proliferation site of the hair follicle follows the pattern of the B2AR expression. It is surprised B2AR concentrated in the bulb region in the mid and late anagen, while chemical sympathectomy has no effect on the hair growth modulation at these stages. This result can be explained by the self-produce NE from the keratinocytes (106). It can be assumed that once hair follicle extends to the adipocytes layer, the water-soluble NE from SN can't diffuse to the B2AR on the bulb. Only the keratinocytes in the bulb can paracrine or autocrine the NE to itself. Further studies will need to investigate if bulb keratinocytes have the ability to produce NE as well and if the NE has the function in these B2AR expression area.

doi:10.6342/NTU201701146

4.2 SN direct effect on the hair growth

Norepinephrine (NE) was believed to decrease the keratinocytes proliferation rate. Dr. Ole Petter Fraas Clausen investigated the basal epidermal cells accelerated its cell cycle from S phase to G2 phase, and the cell cycle was arrested at prophase after i.p. injection of 10μg adrenalin (83). Elaine K. Orenberg also demonstrated the keratinocytes proliferation was interrupted with BAR agonist, isoproterenol, treatment (85). In the previous study, isoproterenol enhanced mouse embryonic stem cells into the cardiac cells and enhanced human induced pluripotent stem cells (iPS) differentiating into mesodermal progenitor cells (107, 108). Further studies on wound healing, B2AR knockout or B2AR antagonist enhanced the keratinocytes motility and promoted cell proliferation (78, 79). Overall, SN was believed to promote the differentiation of the stem cells and inhibit the cell proliferation rate. However, different types of cell have different effect (88, 90).

According to my qPCR result, bulge didn't show any significant difference in the Wnt/ ß-catenin pathway after SN was depleted. But the inhibiting factor BMP4 has been stimulated in the bulge at early anagen entry (Figure 4.1). BMP4 were involved in the hair growth initiation (109). This outcome showed that SN depletion results in the change of the niche around the bulge which turns out repressing the onset of hair growth. At the SN depletion condition, hair follicle needs more activating signals to surpass the inhibiting signal. The threshold of the HFSCs activation is elevated. The hair cycle is blocked at telogen through spontaneous telogen-anagen transition.

doi:10.6342/NTU201701146

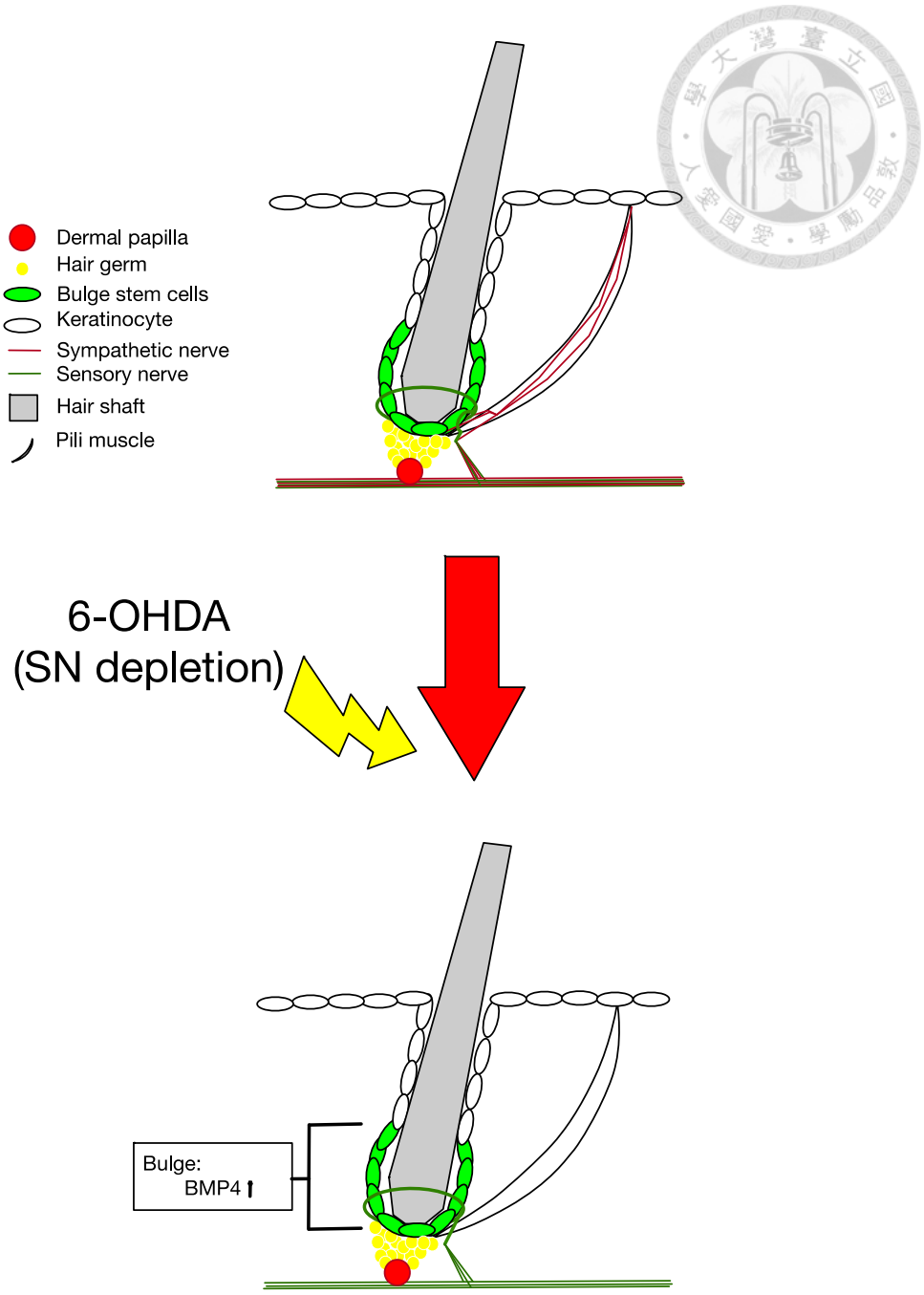

Figure 4.1 The SN-depletion effect on the *BMP4* expression in bulge

doi:10.6342/NTU201701146

At the germ, the level of ß-catenin, and Axin2 declines at SN depleted region. This raises the suspect to the direct influence on hair growth by NE. The NE was investigated to increase the Wnt member ß-catenin (94). Experimental data also suggested Wnt/ß-catenin pathway is enhanced in the immature human $CD34^+$ cells (110). This result is discovered in both bulge and secondary hair germ stem cells (Figure 4.2). The upstream, B2AR, only performed a significant change in the bulge rather than hair germ after the SN denervation. The level of B2AR expression increased after the SN denervation. This may result from the sensitization. Dopamine2 receptor increases its density to respond to the chemical denervation, by 6-OHDA, in striatum (111). This phenomenon demonstrated the importance of B2AR to bulge stem cells compared to germ. If NE is partial supplier to the ß-catenin pathway, this explain my two SN denervation experiment outcomes: 1) the block of hair growth when SN was depleted at telogen, and 2) the delay of hair growth when SN was depleted at early anagen. In the anagen-telogen transition, the bulge stem cells are activated and migrate down to the hair germ then it proliferates to start the hair cycle (105). Without the partial supplies of ß-catenin signaling, the hair cycle was block in the end. On the other side, in the anagen, the bulge stem cells are responsible for the hair elongation. The bulge stem cells migrate down to the upper bulge and have the parallel proliferation to the hair growth direction (8, 9). The depletion of SN in the early stage of hair cycle interrupted the elongation. Therefore, it might be the reason why the hair follicle had a slower growth rate than the SN non-depleted region.

doi:10.6342/NTU201701146

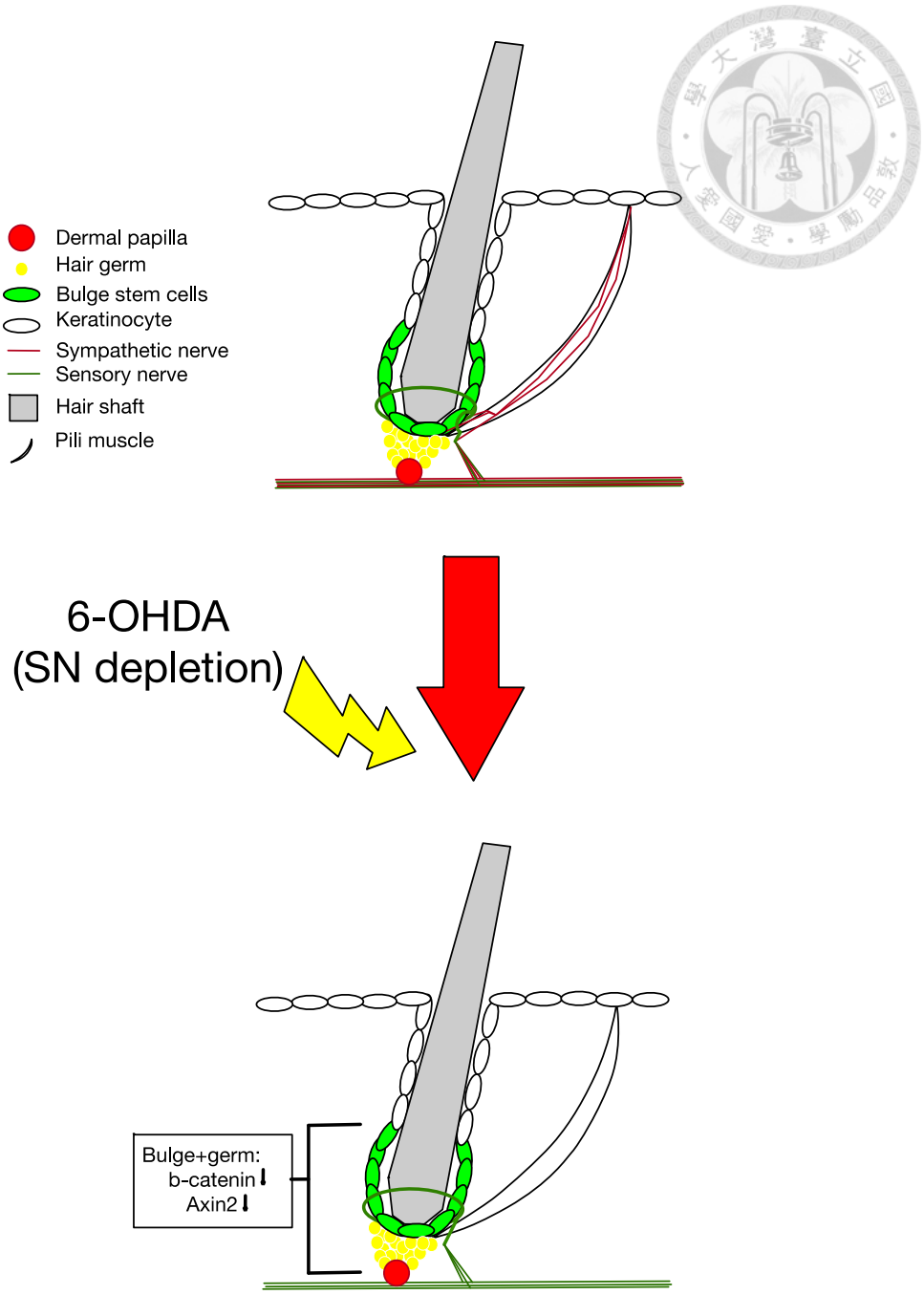

Figure 4.2 The SN-depletion effect on the *Wnt/ ß-catenin* pathway in HFSCs

doi:10.6342/NTU201701146

4.3 SN indirect effect on hair growth

With the discovery of B2AR combined with the ISO-induced hair growth result, NE was considered as the candidate neurotransmitter that responsible for the block and delay of hair cycle after SN depletion. However, the mechanism of how NE stimulate the hair growth has left unknown. According to our result of SN depletion at different stages, SN was investigated to get involved in the hair follicle telogen-anagen transition and early anagen-mid anagen elongation. Although qPCR data revealed, at the early anagen, SN depletion has no effect on Wnt/ß-catenin pathway, the hedgehog signaling pathway*, gli1,* and *gli2*, plunged at the SN depletion region (Figure 4.3). In the hedgehog family, shh is required for hair growth (112). Shh is derived from sensory nerve and can modulate HFSCs activity (32, 113). SN doesn't produce shh signaling proteins. This outcome may be proposed SN indirectly modulate the expression of Shh from sensory nerve to control the beginning of the hair growth. Sympathetic nerve has been investigated to modulate the renal nerve activity through α1 and α2-adrenoceptor on the sensory nerve. Sensory nerve produces PGE2 and substance P under NE stimulation (114). Similar result exhibited in germ. The level of Gli2 dropped at the SN depletion model, while the raised level of Gli1 in germ is still unknown. More experiment is required to realize the influence of SN on sensory nerve behavior.

doi:10.6342/NTU201701146

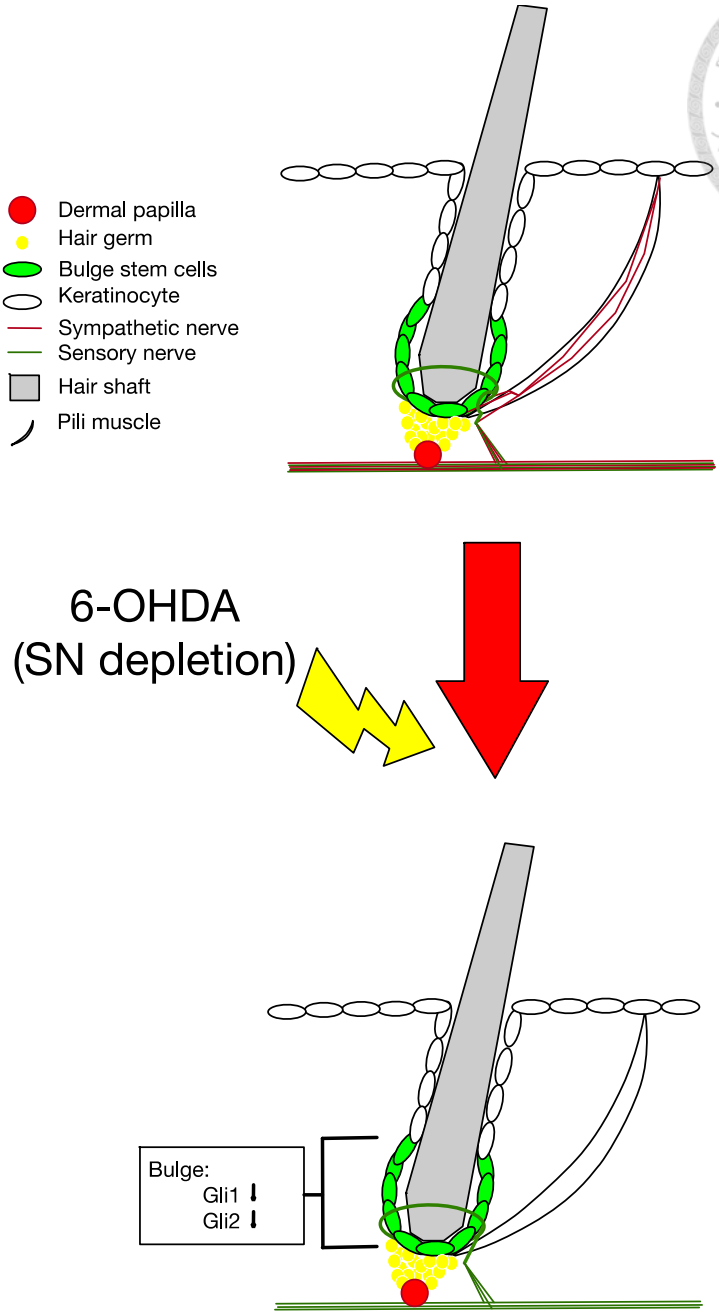

Figure 4.3 The SN-depletion effect on the *gli1*, and *gli2* expression in bulge

doi:10.6342/NTU201701146

SN can also secrete neuropeptide Y (NPY) (115). High dose of NPY promotes the adipocytes differentiation through the PPAPr activation (116). The differentiation of adipocytes was also investigated to partake in hair growth (7). This might be the other plausible pathway on how SN affect hair growth. Nevertheless, the sensory nerve can also secrete the NPY to promote the differentiation of bone marrow mesenchymal stem cells (BMSCs) through the canonical Wnt signaling (117). Therefore, SN may regulate the hair growth through NPY secretion. But NPY from sensory nerve should have some compensatory effect in that only SN depletion should have dominant hair cycle block.

4.4 Relationship between SN and trauma-induced hair cycle

In the first two hair cycle in mouse, the hair cycle synchronized in the back between different individuals at the same time. The prevailing thought of such phenomenon is the circadian rhythm. At first hand, mice sense the light from the ipRGCs. Then, the optic nerve transmits the luminescence signal to the suprachiasmatic nucleus (SCN). The CNS modulate the peripheral tissue clock through hypothalamic-pituitary-adrenal (HPA) axis, ANS, body temperature. The circadian oscillation of hematopoietic stem cell (HSC) recruitment was believed to be responsible for adrenergic nerve (104). SN down-regulates the Cxcl2 and reduce Sp1 for HSC mobilization and then attracts the HSC egress from bone marrow (71, 73). It has been revealed that adrenergic neural input controls the lymphocyte trafficking through Wnt signaling (69, 110). These evidences combined with the oscillation of SN fibers through the hair cycle and the early hair development in the high SN endings density region in rat render the hypothesis that the SN may be the liaison between follicles and SCN and each follicle (31, 99). We use the CsA, an immunosuppressant, to induce a hair wave to test if SN manages the hair cycle signal transduction. The result showed a bypassed hair wave in

doi:10.6342/NTU201701146

the SN depletion region. This gives an insight of that circadian rhythm at skin was modulated under adrenergic control.

Waxing induces the hair cycle with an SN-independent mechanism. The hair performed synchronized hair growth with or without SN depletion. This result is rational. After depilation of the hair follicle at telogen, the cells, K6+ keratinocytes, resides under the club hair was ruptured. These cells expressed highly amount of BMP to inhibit the hair follicle cell proliferation. Once these cell population is devastated, the BMP plunges drastically (9). Hair germ, then, proliferates right after the operation (47). In our hypothesis concluded from the result, the existence of SN provides the permissive niche for the hair follicle to be in the ready state to progress the telogen-anagen transition. Without SN, in the normal condition, the hair cycle will be arrested in telogen. However, with the aberrant low level of BMP-induced by waxing, SN takes the minor role in the control of hair cycle progression.

doi:10.6342/NTU201701146

Chapter 5 Future work

In this study, I identified that telogen-anagen transition is under adrenergic modulation (Figure 5.1). After the denervation of the SN in the skin, the HFSCs turned to a much quiescent state. In my data, this phenomenon was observed to be related to the adrenergic control of Wnt and BMP level.

The future work can be focused on realizing the SN effect on the surrounding cells, fibroblasts, dermal papilla, sensory nerve, adipocytes, etc (Figure 5.2). More neurotransmitters from SN can be investigated to disclose detail mechanism on the how SN affect the hair growth. NPY is a candidate in exploring the relation among SN, adipocytes, and hair follicle. In this study, the level *gli1* and *gli2* have significant decline in bulge and germ at the SN-depletion site. This means the production of hedgehog ligand has decreased in the low concentration of NE environment. The further studied can look into the how NE affects the Hedgehog signaling. The already known Hedgehog signaling in hair follicls is desert hedgehhog (Dhh) and Shh which are produced by dermal papilla and sensory nerve respectively(32, 118). Cycline D1 can also be investigated to understand the NE effect on germ and bulge cell proliferation.

doi:10.6342/NTU201701146

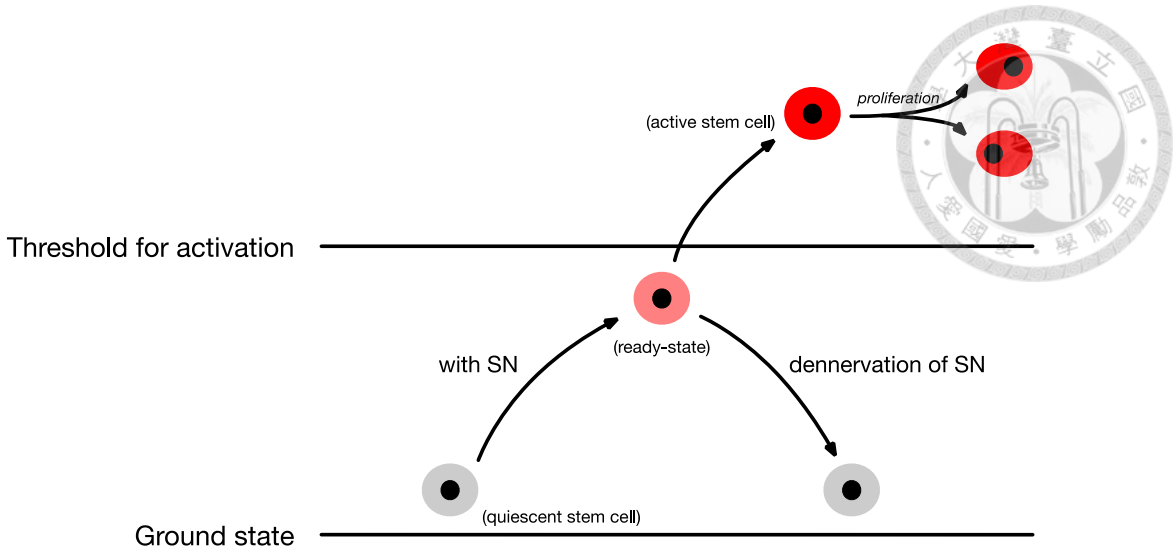

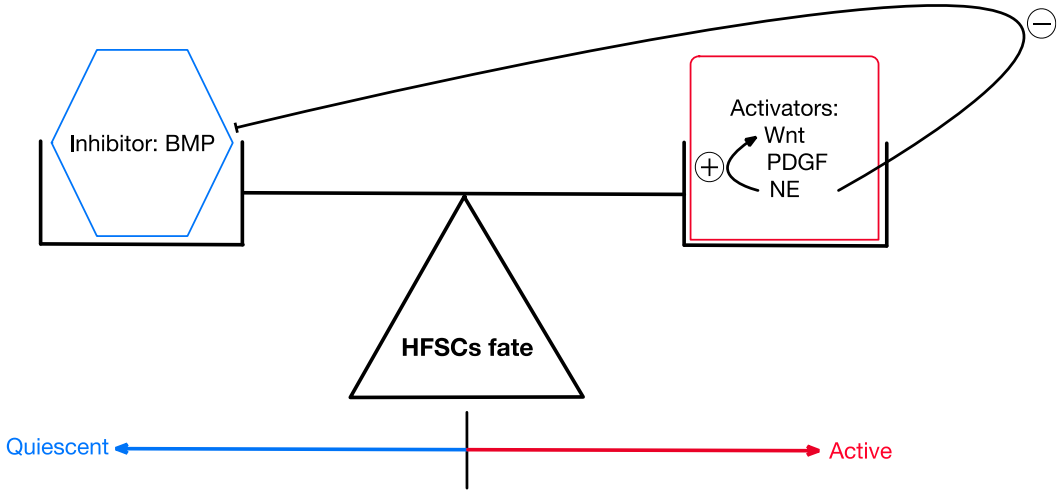

Figure 5.1 SN effect on creating a permission niche in the skin.

doi:10.6342/NTU201701146

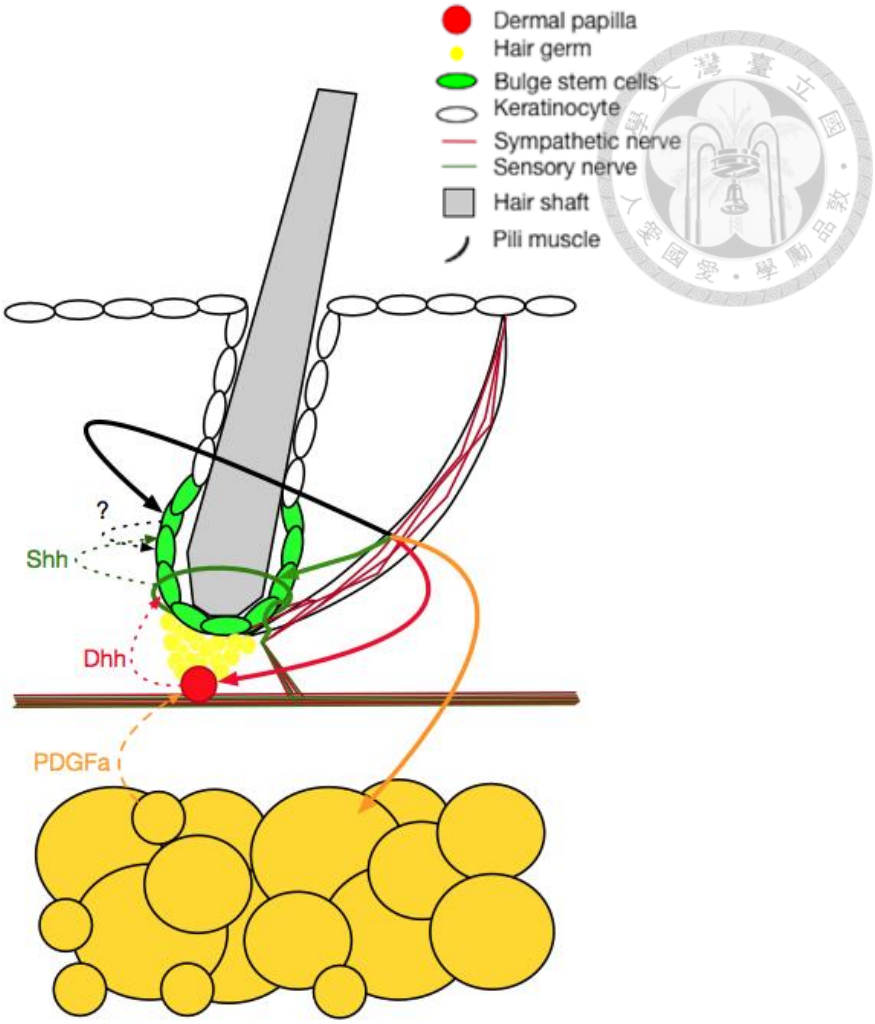

Figure 5.2 Possible pathways of adrenergic control on hair cycle

doi:10.6342/NTU201701146

References

1. Ovaere P, Lippens S, Vandenabeele P, & Declercq W (2009) The emerging roles of serine protease cascades in the epidermis. *Trends Biochem Sci* 34(9):453-463.
2. Bensouilah J BP (2006) Architecture and Function. *Bensouilah J, Buck P (eds) Aromadermatology*.
3. Schmidt-Ullrich R & Paus R (2005) Molecular principles of hair follicle induction and morphogenesis. *Bioessays* 27(3):247-261.
4. Schneider MR, Schmidt-Ullrich R, & Paus R (2009) The hair follicle as a dynamic miniorgan. *Curr Biol* 19(3):R132-142.
5. Stenn KS & Paus R (2001) Controls of hair follicle cycling. *Physiol Rev* 81(1):449-494.
6. Chen CC, Plikus MV, Tang PC, Widelitz RB, & Chuong CM (2016) The Modulatable Stem Cell Niche: Tissue Interactions during Hair and Feather Follicle Regeneration. *J Mol Biol* 428(7):1423-1440.
7. Festa E*, et al.* (2011) Adipocyte lineage cells contribute to the skin stem cell niche to drive hair cycling. *Cell* 146(5):761-771.
8. Panteleyev AA, Jahoda CA, & Christiano AM (2001) Hair follicle predetermination. *J Cell Sci* 114(Pt 19):3419-3431.
9. Hsu YC, Pasolli HA, & Fuchs E (2011) Dynamics between stem cells, niche, and progeny in the hair follicle. *Cell* 144(1):92-105.
10. Solanas G & Benitah SA (2013) Regenerating the skin: a task for the heterogeneous stem cell pool and surrounding niche. *Nat Rev Mol Cell Biol* 14(11):737-748.
11. Lindner G*, et al.* (1997) Analysis of apoptosis during hair follicle regression (catagen). *Am J Pathol* 151(6):1601-1617.
12. Greco V*, et al.* (2009) A two-step mechanism for stem cell activation during hair regeneration. *Cell Stem Cell* 4(2):155-169.
13. Ito M, Kizawa K, Hamada K, & Cotsarelis G (2004) Hair follicle stem cells in the lower bulge form the secondary germ, a biochemically distinct but functionally equivalent progenitor cell population, at the termination of catagen. *Differentiation* 72(9-10):548-557.
14. Rompolas P*, et al.* (2012) Live imaging of stem cell and progeny behaviour in physiological hair-follicle regeneration. *Nature* 487(7408):496-499.
15. Legue E & Nicolas JF (2005) Hair follicle renewal: organization of stem cells in the matrix and the role of stereotyped lineages and behaviors. *Development* 132(18):4143-4154.
16. Rompolas P, Mesa KR, & Greco V (2013) Spatial organization within a niche as a determinant of stem-cell fate. *Nature* 502(7472):513-518.
17. Sequeira I & Nicolas JF (2012) Redefining the structure of the hair follicle by 3D clonal analysis. *Development* 139(20):3741-3751.
18. HB. C (1954) Growth of hair. *Physiol Rev* 34(1):113-126.
19. Muller-Rover S*, et al.* (2001) A comprehensive guide for the accurate classification of murine hair follicles in distinct hair cycle stages. *J Invest Dermatol* 117(1):3-15.

doi:10.6342/NTU201701146

20. Alonso L & Fuchs E (2006) The hair cycle. *J Cell Sci* 119(Pt 3):391-393.
21. Plikus MV & Chuong CM (2008) Complex hair cycle domain patterns and regenerative hair waves in living rodents. *J Invest Dermatol* 128(5):1071-1080.
22. Chase HB & Eaton GJ (1959) The growth of hair follicles in waves. *Ann N Y Acad Sci* 83:365-368.
23. Kulessa H, Turk G, & Hogan BL (2000) Inhibition of Bmp signaling affects growth and differentiation in the anagen hair follicle. *EMBO J* 19(24):6664-6674.
24. Plikus MV*, et al.* (2008) Cyclic dermal BMP signalling regulates stem cell activation during hair regeneration. *Nature* 451(7176):340-344.
25. Reddy S*, et al.* (2001) Characterization of Wnt gene expression in developing and postnatal hair follicles and identification of Wnt5a as a target of Sonic hedgehog in hair follicle morphogenesis. *Mech Dev* 107(1-2):69-82.
26. Tumbar T*, et al.* (2004) Defining the epithelial stem cell niche in skin. *Science* 303(5656):359-363.
27. Zhang Y*, et al.* (2009) Reciprocal requirements for EDA/EDAR/NF-kappaB and Wnt/beta-catenin signaling pathways in hair follicle induction. *Dev Cell* 17(1):49-61.
28. Oshimori N & Fuchs E (2012) Paracrine TGF-beta signaling counterbalances BMP-mediated repression in hair follicle stem cell activation. *Cell Stem Cell* 10(1):63-75.
29. Huelsken J, Vogel R, Erdmann B, Cotsarelis G, & Birchmeier W (2001) beta-Catenin controls hair follicle morphogenesis and stem cell differentiation in the skin. *Cell* 105(4):533-545.
30. Hansen LS, Coggle JE, Wells J, & Charles MW (1984) The influence of the hair cycle on the thickness of mouse skin. *Anat Rec* 210(4):569-573.
31. Botchkarev VA, Peters EM, Botchkareva NV, Maurer M, & Paus R (1999) Hair cycle-dependent changes in adrenergic skin innervation, and hair growth modulation by adrenergic drugs. *J Invest Dermatol* 113(6):878-887.
32. Brownell I, Guevara E, Bai CB, Loomis CA, & Joyner AL (2011) Nerve-derived sonic hedgehog defines a niche for hair follicle stem cells capable of becoming epidermal stem cells. *Cell Stem Cell* 8(5):552-565.
33. Wang LC1 LZ, Gambardella L, Delacour A, Shapiro R, Yang J, Sizing I, Rayhorn P, Garber EA, Benjamin CD, Williams KP, Taylor FR, Barrandon Y, Ling L, Burkly LC. (2000) Conditional Disruption of Hedgehog Signaling Pathway De®nes its Critical Role in Hair Development and Regeneration. *J Invest Dermatol* 114(5):901-908.
34. Paladini RD, Saleh J, Qian C, Xu GX, & Rubin LL (2005) Modulation of hair growth with small molecule agonists of the hedgehog signaling pathway. *J Invest Dermatol* 125(4):638-646.
35. Petrova R & Joyner AL (2014) Roles for Hedgehog signaling in adult organ homeostasis and repair. *Development* 141(18):3445-3457.
36. Martin CM, Southwick EG, & Maibach HI (1973) Propranolol induced alopecia. *Am Heart J* 86(2):236-237.
37. Kobayasi S, Okuyama F, & Takagi K (1958) Experimental studies on the hemitrichosis and the nervous influences on the hair growth. *Acta Neuroveg (Wien)* 18(1-4):169-190.

doi:10.6342/NTU201701146

38. Asada-Kubota M (1995) Inhibition of hair growth by subcutaneous injection of a sympathetic neurotoxin, 6-hydroxydopamine in neonatal mice. *Anat Embryol (Berl)* 191(5):407-414.
39. Kong Y, Liu Y, Pan L, Cheng B, & Liu H (2016) Norepinephrine Regulates Keratinocyte Proliferation to Promote the Growth of Hair Follicles. *Cells Tissues Organs*.
40. Peters EM, Maurer M, Botchkarev VA, Gordon DS, & Paus R (1999) Hair growth-modulation by adrenergic drugs. *Exp Dermatol* 8(4):274-281.
41. Castellana D, Paus R, & Perez-Moreno M (2014) Macrophages contribute to the cyclic activation of adult hair follicle stem cells. *PLoS Biol* 12(12):e1002002.
42. Ali N*, et al.* (2017) Regulatory T Cells in Skin Facilitate Epithelial Stem Cell Differentiation. *Cell* 169(6):1119-1129 e1111.
43. Gay D*, et al.* (2013) Fgf9 from dermal gammadelta T cells induces hair follicle neogenesis after wounding. *Nat Med* 19(7):916-923.
44. Cipolletta D*, et al.* (2012) PPAR-gamma is a major driver of the accumulation and phenotype of adipose tissue Treg cells. *Nature* 486(7404):549-553.
45. Villalta SA*, et al.* (2014) Regulatory T cells suppress muscle inflammation and injury in muscular dystrophy. *Sci Transl Med* 6(258):258ra142.
46. Nosbaum A*, et al.* (2016) Cutting Edge: Regulatory T Cells Facilitate Cutaneous Wound Healing. *J Immunol* 196(5):2010-2014.
47. Ibrahim L & Wright EA (1975) The growth of rats and mice vibrissae under normal and some abnormal conditions. *J Embryol Exp Morphol* 33(4):831-844.
48. Silver AF & Chase HB (1977) The Incorporation of Tritiated Uridine in Hair Germ and Dermal Papilla during Dormancy (Telogen) and Activation (Early Anagen). *Journal of Investigative Dermatology* 68(4):201-205.
49. T.D. L (1934) Studies on the expression of genetic hairlessness in the house mouse. *J. Exp. Zoöl* 68:501-518.
50. Gafter-Gvili A, Sredni B, Gal R, Gafter U, & Kalechman Y (2003) Cyclosporin A-induced hair growth in mice is associated with inhibition of calcineurin-dependent activation of NFAT in follicular keratinocytes. *Am J Physiol Cell Physiol* 284(6):C1593-1603.
51. Maurer M, Handjiski B, & Paus R (1997) Hair growth modulation by topical immunophilin ligands: induction of anagen, inhibition of massive catagen development, and relative protection from chemotherapy-induced alopecia. *Am J Pathol* 150(4):1433-1441.
52. Xu W, Fan W, & Yao K (2012) Cyclosporine A stimulated hair growth from mouse vibrissae follicles in an organ culture model. *J Biomed Res* 26(5):372-380.
53. Paus R, Handjiski B, Czarnetzki BM, & Eichmuller S (1994) A murine model for inducing and manipulating hair follicle regression (catagen): effects of dexamethasone and cyclosporin A. *J Invest Dermatol* 103(2):143-147.
54. Paus R, Handjiski B, Eichmuller S, & Czarnetzki BM (1994) Chemotherapy-induced alopecia in mice. Induction by cyclophosphamide, inhibition by cyclosporine A, and modulation by dexamethasone. *Am J Pathol* 144(4):719-734.
55. Kim CD*, et al.* (2008) Induction of synapse associated protein 102 expression in cyclosporin A-stimulated hair growth. *Exp Dermatol* 17(8):693-699.

doi:10.6342/NTU201701146

56. Gafter-Gvili A, Kalechman Y, Sredni B, Gal R, & Gafter U (2004) Cyclosporin A-induced hair growth in mice is associated with inhibition of hair follicle regression. *Arch Dermatol Res* 296(6):265-269.
57. de Arriba G, Calvino M, Benito S, & Parra T (2013) Cyclosporine A-induced apoptosis in renal tubular cells is related to oxidative damage and mitochondrial fission. *Toxicol Lett* 218(1):30-38.
58. Lan S*, et al.* (2015) Cyclosporine A increases hair follicle growth by suppressing apoptosis-inducing factor nuclear translocation: a new mechanism. *Fundam Clin Pharmacol* 29(2):191-203.
59. Norberg E, Orrenius S, & Zhivotovsky B (2010) Mitochondrial regulation of cell death: processing of apoptosis-inducing factor (AIF). *Biochem Biophys Res Commun* 396(1):95-100.
60. Roue G*, et al.* (2003) Mitochondrial dysfunction in CD47-mediated caspase-independent cell death: ROS production in the absence of cytochrome c and AIF release. *Biochimie* 85(8):741-746.
61. Zhu C*, et al.* (2007) Cyclophilin A participates in the nuclear translocation of apoptosis-inducing factor in neurons after cerebral hypoxia-ischemia. *J Exp Med* 204(8):1741-1748.
62. Zupanska A, Dziembowska M, Ellert-Miklaszewska A, Gaweda-Walerych K, & Kaminska B (2005) Cyclosporine a induces growth arrest or programmed cell death of human glioma cells. *Neurochem Int* 47(6):430-441.
63. O'Donnell J, Zeppenfeld D, McConnell E, Pena S, & Nedergaard M (2012) Norepinephrine: a neuromodulator that boosts the function of multiple cell types to optimize CNS performance. *Neurochem Res* 37(11):2496-2512.
64. Soeda J*, et al.* (2014) The beta-adrenoceptor agonist isoproterenol rescues acetaminophen-injured livers through increasing progenitor numbers by Wnt in mice. *Hepatology* 60(3):1023-1034.
65. Oben JA*, et al.* (2003) Sympathetic nervous system inhibition increases hepatic progenitors and reduces liver injury. *Hepatology* 38(3):664-673.
66. Oben JA & Diehl AM (2004) Sympathetic nervous system regulation of liver repair. *Anat Rec A Discov Mol Cell Evol Biol* 280(1):874-883.
67. Mutlu GM & Factor P (2008) Alveolar epithelial beta2-adrenergic receptors. *Am J Respir Cell Mol Biol* 38(2):127-134.
68. Salathe M (2002) Effects of beta-agonists on airway epithelial cells. *J Allergy Clin Immunol* 110(6 Suppl):S275-281.
69. Suzuki K, Hayano Y, Nakai A, Furuta F, & Noda M (2016) Adrenergic control of the adaptive immune response by diurnal lymphocyte recirculation through lymph nodes. *J Exp Med* 213(12):2567-2574.
70. Sun F*, et al.* (2015) beta2-Adrenoreceptor-Mediated Proliferation Inhibition of Embryonic Pluripotent Stem Cells. *J Cell Physiol* 230(11):2640-2646.
71. Mendez-Ferrer S, Battista M, & Frenette PS (2010) Cooperation of beta(2)- and beta(3)-adrenergic receptors in hematopoietic progenitor cell mobilization. *Ann N Y Acad Sci* 1192:139-144.
72. Arranz L*, et al.* (2014) Neuropathy of haematopoietic stem cell niche is essential for myeloproliferative neoplasms. *Nature* 512(7512):78-81.
73. Katayama Y*, et al.* (2006) Signals from the sympathetic nervous system regulate hematopoietic stem cell egress from bone marrow. *Cell* 124(2):407-421.

doi:10.6342/NTU201701146

74. Gillbro JM, Marles LK, Hibberts NA, & Schallreuter KU (2004) Autocrine catecholamine biosynthesis and the beta-adrenoceptor signal promote pigmentation in human epidermal melanocytes. *J Invest Dermatol* 123(2):346-353.
75. Ma M*, et al.* (2015) Effects of norepinephrine on proliferation and apoptosis of neonatal cardiac fibroblasts in rats. *Zhonghua Xin Xue Guan Bing Za Zhi* 43(6):542-547.
76. Lorenz J*, et al.* (2016) Norepinephrine modulates osteoarthritic chondrocyte metabolism and inflammatory responses. *Osteoarthritis Cartilage* 24(2):325-334.
77. Sivamani RK*, et al.* (2014) Acute wounding alters the beta2-adrenergic signaling and catecholamine synthetic pathways in keratinocytes. *J Invest Dermatol* 134(8):2258-2266.
78. Pullar CE*, et al.* (2012) beta2AR antagonists and beta2AR gene deletion both promote skin wound repair processes. *J Invest Dermatol* 132(8):2076-2084.
79. Souza BR, Santos JS, & Costa AM (2006) Blockade of beta1- and beta2-adrenoceptors delays wound contraction and re-epithelialization in rats. *Clin Exp Pharmacol Physiol* 33(5-6):421-430.
80. Kimura K, Ieda M, & Fukuda K (2012) Development, maturation, and transdifferentiation of cardiac sympathetic nerves. *Circ Res* 110(2):325-336.
81. Wang L*, et al.* (2014) A conserved axon type hierarchy governing peripheral nerve assembly. *Development* 141(9):1875-1883.
82. Liu LY, Zhang H, Pan J, & Pen A (2005) The existence of a linear system consisting of sympathetic endings in rat skin. *Anat Embryol (Berl)* 210(2):91-100.
83. Clausen OPF, Thorud E, & Iversen OH (1982) Adrenalin Has Differential Effects of Epidermal Cell Cycle Progression in Mice. *Journal of Investigative Dermatology* 78(6):472-476.
84. Schallreuter KU*, et al.* (1995) Catecholamines in human keratinocyte differentiation. *J Invest Dermatol* 104(6):953-957.
85. Orenberg EK & Wilkinson DI (1982) Effect of beta-adrenergic receptor blockade or refractoriness induced by isoproterenol on growth of keratinocytes in vitro. *Br J Dermatol* 107 Suppl 23:119-124.
86. Sivamani RK, Lam ST, & Isseroff RR (2007) Beta adrenergic receptors in keratinocytes. *Dermatol Clin* 25(4):643-653, x.
87. Orenberg EK, Pfendt EA, & Wilkinson DI (1983) Characterization of alpha- and beta-adrenergic agonist stimulation of adenylate cyclase activity in human epidermal keratinocytes in vitro. *J Invest Dermatol* 80(6):503-507.
88. Kim N*, et al.* (2006) Site specific differential activation of ras/raf/ERK signaling in rabbit isoproterenol-induced left ventricular hypertrophy. *Biochim Biophys Acta* 1763(10):1067-1075.
89. Shenoy SK*, et al.* (2006) beta-arrestin-dependent, G protein-independent ERK1/2 activation by the beta2 adrenergic receptor. *J Biol Chem* 281(2):1261-1273.
90. Zheng M, Hou R, Han Q, & Xiao RP (2004) Different regulation of ERK1/2 activation by beta-adrenergic receptor subtypes in adult mouse cardiomyocytes. *Heart Lung Circ* 13(2):179-183.

doi:10.6342/NTU201701146

91. Chen J, Hoffman BB, & Isseroff RR (2002) Beta-adrenergic receptor activation inhibits keratinocyte migration via a cyclic adenosine monophosphate-independent mechanism. *J Invest Dermatol* 119(6):1261-1268.
92. Pullar CE, Chen J, & Isseroff RR (2003) PP2A activation by beta2-adrenergic receptor agonists: novel regulatory mechanism of keratinocyte migration. *J Biol Chem* 278(25):22555-22562.
93. Li W*, et al.* (2013) Epidermal adrenergic signaling contributes to inflammation and pain sensitization in a rat model of complex regional pain syndrome. *Pain* 154(8):1224-1236.
94. Hino S, Tanji C, Nakayama KI, & Kikuchi A (2005) Phosphorylation of beta-catenin by cyclic AMP-dependent protein kinase stabilizes beta-catenin through inhibition of its ubiquitination. *Mol Cell Biol* 25(20):9063-9072.
95. Boyce ST & Ham RG (1983) Calcium-regulated differentiation of normal human epidermal keratinocytes in chemically defined clonal culture and serum-free serial culture. *J Invest Dermatol* 81(1 Suppl):33s-40s.
96. Hennings H*, et al.* (1980) Calcium regulation of growth and differentiation of mouse epidermal cells in culture. *Cell* 19(1):245-254.
97. Maurer M, Peters EM, Botchkarev VA, & Paus R (1998) Intact hair follicle innervation is not essential for anagen induction and development. *Arch Dermatol Res* 290(10):574-578.
98. Blum D*, et al.* (2001) Molecular pathways involved in the neurotoxicity of 6-OHDA, dopamine and MPTP: contribution to the apoptotic theory in Parkinson's disease. *Prog Neurobiol* 65(2):135-172.
99. Liu LY, Guo DS, Xin XY, & Fang J (2008) Observation of a system of linear loops formed by re-growing hairs on rat skin. *Anat Rec (Hoboken)* 291(7):858-868.
100. Roth S & Kummer W (1994) A quantitative ultrastructural investigation of tyrosine hydroxylase-immunoreactive axons in the hairy skin of the guinea pig. *Anat Embryol (Berl)* 190(2):155-162.
101. Eaton HBCaGJ (1959) The growth of hair follicles in waves. *Annals of the New York Academy of Sciences* 83(1):365-368.
102. Liapakis G, Chan WC, Papadokostaki M, & Javitch JA (2004) Synergistic contributions of the functional groups of epinephrine to its affinity and efficacy at the beta2 adrenergic receptor. *Mol Pharmacol* 65(5):1181-1190.
103. Steinkraus V*, et al.* (1996) Autoradiographic mapping of beta-adrenoceptors in human skin. *Arch Dermatol Res* 288(9):549-553.
104. Scheiermann C*, et al.* (2012) Adrenergic nerves govern circadian leukocyte recruitment to tissues. *Immunity* 37(2):290-301.
105. Zhang YV, Cheong J, Ciapurin N, McDermitt DJ, & Tumbar T (2009) Distinct self-renewal and differentiation phases in the niche of infrequently dividing hair follicle stem cells. *Cell Stem Cell* 5(3):267-278.
106. Schallreuter KU*, et al.* (1992) Production of catecholamines in the human epidermis. *Biochem Biophys Res Commun* 189(1):72-78.
107. Ishizuka T, Goshima H, Ozawa A, & Watanabe Y (2014) Involvement of beta-adrenoceptors in the differentiation of human induced pluripotent stem cells into mesodermal progenitor cells. *Eur J Pharmacol* 740:28-34.

doi:10.6342/NTU201701146

108. Yan L*, et al.* (2011) Beta-adrenergic signals regulate cardiac differentiation of mouse embryonic stem cells via mitogen-activated protein kinase pathways. *Dev Growth Differ* 53(6):772-779.
109. Sennett R & Rendl M (2012) Mesenchymal-epithelial interactions during hair follicle morphogenesis and cycling. *Semin Cell Dev Biol* 23(8):917-927.
110. Spiegel A*, et al.* (2007) Catecholaminergic neurotransmitters regulate migration and repopulation of immature human CD34+ cells through Wnt signaling. *Nat Immunol* 8(10):1123-1131.
111. Cai G, Wang HY, & Friedman E (2002) Increased dopamine receptor signaling and dopamine receptor-G protein coupling in denervated striatum. *J Pharmacol Exp Ther* 302(3):1105-1112.
112. Sato N, Leopold PL, & Crystal RG (1999) Induction of the hair growth phase in postnatal mice by localized transient expression of Sonic hedgehog. *J Clin Invest* 104(7):855-864.
113. Zhao H*, et al.* (2014) Secretion of shh by a neurovascular bundle niche supports mesenchymal stem cell homeostasis in the adult mouse incisor. *Cell Stem Cell* 14(2):160-173.
114. Kopp UC, Cicha MZ, Smith LA, Mulder J, & Hokfelt T (2007) Renal sympathetic nerve activity modulates afferent renal nerve activity by PGE2-dependent activation of alpha1- and alpha2-adrenoceptors on renal sensory nerve fibers. *Am J Physiol Regul Integr Comp Physiol* 293(4):R1561-1572.
115. Lundberg JM, Terenius L, Hokfelt T, & Goldstein M (1983) High levels of neuropeptide Y in peripheral noradrenergic neurons in various mammals including man. *Neurosci Lett* 42(2):167-172.
116. Tang HN*, et al.* (2015) Dose-dependent effects of neuropeptide Y on the regulation of preadipocyte proliferation and adipocyte lipid synthesis via the PPARgamma pathways. *Endocr J* 62(9):835-846.
117. Liu S*, et al.* (2016) Neuropeptide Y stimulates osteoblastic differentiation and VEGF expression of bone marrow mesenchymal stem cells related to canonical Wnt signaling activating in vitro. *Neuropeptides* 56:105-113.
118. Driskell RR, Giangreco A, Jensen KB, Mulder KW, & Watt FM (2009) Sox2-positive dermal papilla cells specify hair follicle type in mammalian epidermis. *Development* 136(16):2815-2823.

doi:10.6342/NTU201701146